Chemical Engineering Journal Advances 27 (2026) 101295

Contents lists available at ScienceDirect

Chemical Engineering Journal Advances

journal homepage: www.sciencedirect.com/journal/chemical-engineering-journal-advances

Microstructural Thermo-Hydraulic Optimization of Microporous Layers for Enhanced Transport in High-Load PEM Fuel Cells

Akram E. Zeid [a], Sa′ed Rawashdea [a,*], Mohammad R. Almajali [b], Ahmed M. Salem [a], Nathan Kawansson [c]

[a] Marine Engineering Technology, Sharjah Maritime Academy, Sharjah, United Arab Emirates
[b] Defence and Security Program, Rabdan Academy, Abu Dhabi, United Arab Emirates
[c] Maritime Logistics and Supply Chain Management (MLSCM), Sharjah Maritime Academy, Sharjah, United Arab Emirates

ARTICLE INFO

Key words:
Proton Exchange Membrane Fuel Cells (PEMFCs)
Microporous Layer Optimization
Thermo-Hydraulic Transport
Multiphysics Modeling
Water Management

ABSTRACT

The performance of proton exchange membrane fuel cells (PEMFCs) operating at high current densities is severely limited by coupled mass transport, water management, thermal regulation, and hydraulic resistance phenomena occurring within porous transport layers. Among these components, the microporous layer (MPL) plays a critical role in controlling oxygen delivery, liquid water evacuation, heat dissipation, and interfacial transport stability; however, its microstructural optimization under high-load conditions remains insufficiently understood. Therefore, this study develops a comprehensive three-dimensional non-isothermal two-phase multiphysics model to investigate and optimize MPL microstructural characteristics for enhanced PEMFC performance. The model simultaneously couples electrochemical kinetics, multicomponent species transport, liquid water dynamics, porous momentum transport, heat transfer, and membrane hydration behavior under realistic operating conditions. Key MPL parameters, including porosity, thickness, permeability, tortuosity, pore diameter, wettability, and thermal conductivity, were systematically evaluated within a multi-objective thermo-hydraulic optimization framework. The optimized MPL architecture achieved approximately 63% improvement in power density, nearly 74% exergy efficiency, up to 96% water removal effectiveness, and more than 60% reduction in cathode pressure losses compared with the baseline configuration. Furthermore, significant improvements in oxygen accessibility, thermal uniformity, membrane hydration stability, and electrochemical activity distribution were observed. The results demonstrate that coordinated microstructural optimization effectively mitigates transport limitations associated with high-current-density operation and substantially enhances PEMFC efficiency and operational robustness. This work establishes an integrated microstructural design methodology for advanced MPL engineering and provides practical design guidelines for the development of next-generation high-performance PEMFC systems for transportation, stationary power, and clean-energy applications.

1. Introduction

1.1. Background and Motivation

Based on the identified research gap and scientific challenges discussed above, this work develops a comprehensive microstructural thermo-hydraulic optimization framework. The accelerating global demand for clean, reliable, and sustainable energy has intensified the search for advanced energy conversion technologies capable of mitigating greenhouse gas emissions while maintaining high efficiency and operational flexibility. Conventional fossil-fuel-based energy systems continue to dominate global power generation and transportation sectors; however, their environmental consequences, finite resource dependency, and vulnerability to energy security disruptions have significantly strengthened the global transition toward low-carbon alternatives [1–5]. In this context, hydrogen has emerged as a strategically important energy carrier due to its high gravimetric energy density, clean oxidation pathway, and compatibility with renewable energy integration. Among the available hydrogen utilization technologies, electrochemical energy conversion systems-particularly fuel cells-have attracted extensive scientific and industrial interest because of their

* Corresponding author. Dr Sa′ed Rawashdeaa, Sharjah Maritime Academy, United Arab Emirates
E-mail address: saad.alrwashdeh@sma.ac.ae (S. Rawashdea).

https://doi.org/10.1016/j.ceja.2026.101295

Available online 8 June 2026
2666-8211/© 2026 The Author(s). Published by Elsevier B.V. This is an open access article under the CC BY-NC-ND license (http://creativecommons.org/licenses/by-nc-nd/4.0/).

Nomenclature

a_{act}	active surface area density m^{-1}
C	concentration mol m^{-3}
c_p	specific heat J kg^{-1} K^{-1}
D_i	diffusivity m^2 s^{-1}
D_{eff}	effective diffusivity m^2 s^{-1}
D_w	membrane water diffusivity m^2 s^{-1}
E_a	activation energy J mol^{-1}
E_{eq}	equilibrium potential V
E_{th}	thermodynamic potential V
F	Faraday constant C mol^{-1}
i	current density A m^{-2}
j	transfer current density A m^{-3}
j_0	exchange current density A m^{-2}
$J_{(s)}$	Leverett function —
K	permeability m^2
k	thermal conductivity W m^{-1} K^{-1}
k_{rl}	relative permeability —
M_i	molecular weight kg mol^{-1}
N_w	membrane water flux mol m^{-2} s^{-1}
n_d	electro-osmotic drag coefficient —
p	pressure Pa
p_c	capillary pressure Pa
Q	heat source W m^{-3}
R	universal gas constant J mol^{-1} K^{-1}
S_i	species source term kg m^{-3} s^{-1}
s	liquid saturation —
T	temperature K
u	velocity m s^{-1}
V_{cell}	cell voltage V
Y_i	species mass fraction —
α	transfer coefficient —
ε	porosity —
η	activation overpotential V
θ	contact angle degree
κ	proton conductivity S m^{-1}
λ	membrane hydration number —
μ	viscosity Pa·s
ρ	density kg m^{-3}
σ	electrical conductivity S m^{-1}
σ_{lv}	surface tension N m^{-1}
τ	tortuosity —
ϕ_s	solid potential V
ϕ_m	membrane potential V

ability to directly convert chemical energy into electrical power with superior efficiency compared with conventional thermal power systems [3,6–9]. Fuel cells offer silent operation, modular scalability, rapid response, and negligible local pollutant emissions, making them attractive for transportation, stationary power generation, aerospace systems, marine electrification, and distributed clean energy infrastructures. Nevertheless, the practical deployment of fuel cell technologies at large commercial scales remains constrained by durability limitations, cost challenges, and complex transport-related performance degradation mechanisms that become particularly severe under aggressive operating conditions [2,10–13].

The increasing penetration of renewable energy resources and the accelerating global transition toward low-carbon energy systems have intensified interest in hydrogen-based energy technologies as key enablers of future energy sustainability. Recent studies have highlighted the critical role of advanced energy conversion and storage technologies in addressing grid flexibility, renewable intermittency, and carbon reduction objectives. In particular, the integration of hydrogen and fuel-cell technologies has been recognized as an effective pathway for supporting energy-sector decarbonization while improving system reliability and energy security. Furthermore, emerging research has emphasized the importance of developing highly efficient electrochemical energy conversion systems capable of overcoming transport, thermal, and operational limitations that restrict large-scale deployment. These developments reinforce the growing need for advanced PEMFC designs that can deliver higher efficiency, improved durability, and enhanced transport performance under demanding operating conditions, thereby supporting broader global clean-energy and net-zero transition strategies [14,15].

Among the various fuel cell technologies, proton exchange membrane fuel cells (PEMFCs) have emerged as one of the most technologically mature and commercially viable electrochemical systems owing to their relatively low operating temperatures, rapid startup capability, high power density, compact design, and suitability for dynamic load applications. These attributes have made PEMFCs particularly attractive for automotive propulsion, heavy-duty transportation, backup power systems, portable energy platforms, and increasingly, marine decarbonization initiatives [16–20]. Comprehensive reviews by Owejan et al. and colleagues, as well as foundational works by Zhang et al., established the thermodynamic and engineering significance of PEMFC systems while highlighting the dominant role of transport management in practical performance realization. Despite their technological promise, PEMFC performance remains highly sensitive to operating conditions, particularly at elevated current densities where electrochemical demand intensifies and coupled transport phenomena become strongly nonlinear [21–24]. Under such regimes, oxygen depletion, liquid water accumulation, membrane dehydration, temperature non-uniformity, and hydraulic resistance interact simultaneously, often triggering substantial voltage losses and accelerated material degradation. Consequently, enhancing PEMFC performance under high-load operation requires not only improved electrochemical activity but also sophisticated transport architecture engineering capable of maintaining stable multiphysics balance.

The performance limitations of PEMFCs under high current density conditions have been extensively investigated by several researchers, with transport losses consistently identified as dominant constraints once activation losses become comparatively less significant. Seminal theoretical work by Wang et al. established a rigorous framework for understanding coupled electrochemical transport phenomena in PEM fuel cells, demonstrating the intricate interaction between ionic conduction, species diffusion, thermal effects, and water transport. Similarly, studies by Wang and collaborators emphasized that performance deterioration under high-load operation is strongly governed by oxygen transport resistance, cathode flooding, and localized thermal instabilities [25,26]. These challenges become especially pronounced when increased reactant demand exceeds the transport capacity of the porous media, leading to concentration polarization, reactant starvation, and unstable cell voltage behavior. High current density operation is particularly desirable for practical applications because it enables compact system design and higher power output per unit active area; however, this operational advantage simultaneously intensifies transport bottlenecks that conventional PEMFC architectures often struggle to accommodate effectively [18,19,22,25–27].

The porous transport architecture of PEMFCs plays a decisive role in governing internal reactant delivery, product water evacuation, thermal regulation, and mechanical support. This architecture consists primarily of the catalyst layer (CL), microporous layer (MPL), and gas diffusion layer (GDL), each performing distinct but strongly interconnected

transport functions. The catalyst layer serves as the electrochemically active reaction zone, while the gas diffusion layer provides macroscopic gas distribution and structural integrity [6,28–30]. Positioned between these components, the microporous layer acts as a transitional transport interface responsible for redistributing reactants, regulating liquid water transport, smoothing contact resistance, and enhancing thermal communication between adjacent layers. Experimental and modeling studies by Litster and McLean highlighted the critical contribution of porous media architecture to PEMFC performance, emphasizing that internal transport efficiency is highly dependent on morphological design. Further investigations by Bazylak demonstrated the complex multiphase nature of water transport through PEMFC porous structures, revealing that local pore-scale interactions significantly influence global cell behavior [31]. These findings collectively underscore that PEMFC performance cannot be optimized solely through electrochemical improvements without simultaneously addressing the transport architecture that supports reactant and thermal management.

Among the porous transport components, the microporous layer has increasingly been recognized as one of the most influential yet structurally under-optimized elements in PEMFC design. Typically composed of carbon-based porous matrices with hydrophobic additives such as polytetrafluoroethylene (PTFE), the MPL exhibits highly tunable microstructural properties including porosity, pore size distribution, thickness, permeability, tortuosity, wettability, and thermal conductivity [32–35]. These characteristics collectively determine the effectiveness of gas diffusion, capillary-driven liquid transport, thermal dissipation, and hydraulic resistance. Research by Gostick significantly advanced pore-network understanding of PEMFC porous transport behavior, illustrating how pore morphology directly influences saturation dynamics and transport resistance [30,36]. Likewise, investigations by Hasan et al. emphasized the dual role of MPL structures in simultaneously mitigating flooding and preserving membrane hydration [8]. However, modifying one microstructural property often improves one transport mechanism while degrading another; for example, increased hydrophobicity may facilitate water removal but impede membrane hydration, while lower tortuosity may enhance oxygen diffusion at the expense of structural robustness. This intrinsic trade-off makes MPL engineering fundamentally a multi-objective optimization challenge rather than a single-parameter design exercise.

Although extensive literature exists on PEMFC transport optimization, most previous studies have focused predominantly on flow field geometry, catalyst layer enhancement, membrane hydration strategies, or gas diffusion layer modifications, while comparatively fewer investigations have systematically addressed microporous layer microstructural optimization under strongly coupled thermo-hydraulic operating conditions. Several studies have explored isolated MPL parameters; however, many adopted simplified assumptions that neglect the simultaneous interaction between heat transfer, momentum losses, capillary transport, and electrochemical demand [37–41]. Furthermore, much of the literature evaluates PEMFC behavior under moderate operating conditions, whereas practical deployment increasingly requires stable performance at elevated current densities where transport limitations become dominant. The lack of integrated thermo-hydraulic optimization frameworks for MPL design creates a critical knowledge gap, particularly regarding how coupled microstructural variables interact to influence oxygen accessibility, liquid water evacuation, thermal uniformity, and pressure penalties in high-load PEMFC operation. This gap is especially significant because optimizing one transport mechanism in isolation may lead to misleading design conclusions when evaluated within the full multiphysics environment of realistic PEMFC operation. Despite the rapid expansion of hydrogen-related research and increasing emphasis on fuel-cell deployment within future sustainable energy infrastructures, comprehensive studies that simultaneously optimize microporous layer microstructure from thermal, hydraulic, and electrochemical perspectives remain limited. Consequently, further investigation is required to establish integrated design methodologies capable of supporting next-generation high-performance PEMFC system

Recent advances in computational multiphysics modeling and optimization algorithms have created significant opportunities for rational PEMFC porous media engineering. High-fidelity three-dimensional numerical models now enable simultaneous resolution of electrochemical kinetics, multicomponent species transport, thermal energy transfer, multiphase water movement, and momentum conservation within complex fuel cell domains. These computational capabilities provide a physically grounded pathway for exploring transport phenomena beyond the limitations of purely experimental trial-and-error development. Multi-objective optimization methods, including evolutionary algorithms, surrogate-assisted optimization, and Pareto-based design exploration, have demonstrated strong potential in identifying balanced design solutions within competing performance objectives. Nevertheless, the application of such methodologies specifically to MPL microstructural thermo-hydraulic optimization remains comparatively limited, particularly in configurations emphasizing high-load PEMFC operation [27,42–44]. A systematic integration of realistic multiphysics transport modeling with microstructural optimization is therefore essential to establish robust design principles for next-generation PEMFC porous transport architectures.

Recent advances in optimization-based fuel-cell research have increasingly incorporated intelligent optimization algorithms, evolutionary computation techniques, and surrogate-assisted modeling approaches to improve parameter estimation accuracy and computational efficiency. Several studies have demonstrated the effectiveness of advanced optimization strategies for identifying optimal fuel-cell operating parameters and enhancing predictive modeling performance. For example, two-stage Differential Evolution algorithms have been successfully applied for robust PEMFC parameter estimation, while novel metaheuristic approaches such as the Parrot Optimizer have demonstrated improved convergence characteristics and solution quality in fuel-cell optimization problems. Similarly, surrogate-assisted Differential Evolution techniques have been employed to accelerate parameter identification in solid oxide fuel cells (SOFCs), reducing computational effort while maintaining prediction accuracy. More recently, hybrid optimization frameworks integrating Aquila Optimizer and Arithmetic Optimization strategies have shown promising capabilities for PEMFC modeling and parameter extraction by balancing global exploration and local exploitation within complex search spaces. These developments highlight the growing importance of intelligent optimization methodologies in electrochemical energy-system research and reinforce the need for computational frameworks capable of integrating advanced optimization concepts with physically realistic transport modelling [45–48].

Despite these advances, most optimization studies have primarily focused on parameter estimation, model calibration, or operational optimization rather than detailed microstructural transport optimization of PEMFC porous transport layers. Furthermore, relatively few investigations have integrated advanced optimization concepts with comprehensive thermo-hydraulic transport analysis capable of simultaneously evaluating oxygen diffusion, liquid-water transport, thermal regulation, hydraulic resistance, membrane hydration behavior, and exergy performance. The present work contributes to this area by providing a physics-based multiphysics optimization framework specifically focused on microporous layer engineering and coupled transport enhancement under high-current-density operating conditions [49].

In this work, a comprehensive microstructural thermo-hydraulic optimization framework is developed to investigate and enhance the transport performance of microporous layers in high-load proton exchange membrane fuel cells. The study employs an advanced three-dimensional multiphysics modeling approach that couples' electrochemical reaction kinetics, multicomponent reactant transport, liquid water dynamics, heat transfer, and momentum conservation under realistic operating conditions representative of demanding PEMFC

applications. Key MPL microstructural design variables, including porosity, pore morphology, permeability, thickness, tortuosity, wettability behavior, and thermal transport characteristics, are systematically analyzed to quantify their individual and coupled effects on oxygen transport resistance, water management efficiency, thermal uniformity, and hydraulic losses. A multi-objective optimization strategy is implemented to identify balanced MPL configurations capable of simultaneously maximizing reactant accessibility, minimizing flooding susceptibility, improving heat dissipation, and reducing parasitic transport penalties. The outcomes of this work aim to establish physically informed microstructural design guidelines for advanced PEMFC porous transport layers, thereby contributing toward higher power density, enhanced durability, and more stable high-load fuel cell operation.

1.2. Research Gap, Novelty, and Scientific Contribution

Despite substantial advances in proton exchange membrane fuel cell (PEMFC) technology, transport-related losses continue to represent one of the primary obstacles limiting high-current-density operation and long-term system efficiency. Previous investigations have demonstrated that modifications to flow-field geometries, gas diffusion layers (GDLs), catalyst layers, membrane hydration strategies, and porous transport structures can improve individual aspects of PEMFC performance [14,37,40,44,50–55]. However, most available studies have focused on isolated transport mechanisms or single design parameters, thereby providing only a partial understanding of the strongly coupled interactions among oxygen transport, liquid water dynamics, thermal regulation, hydraulic resistance, and electrochemical activity that govern practical PEMFC operation.

Several studies have reported performance improvements through flow-field optimization and reactant distribution enhancement [10,31,32,55–58], while others have focused on porosity engineering and structural modification of gas diffusion layers to improve mass transport behavior [15,30,37]. Similarly, wettability engineering and water management investigations have demonstrated the importance of capillary transport regulation in mitigating cathode flooding and maintaining membrane hydration stability [30,35,40,59–61]. Although these studies have significantly advanced PEMFC understanding, they generally evaluate a limited subset of transport phenomena and rarely consider the simultaneous optimization of multiple microporous layer (MPL) microstructural parameters within a fully coupled thermo-hydraulic environment. Consequently, the complex transport trade-offs associated with high-load PEMFC operation remain insufficiently understood.

Furthermore, recent developments in intelligent optimization algorithms and advanced parameter identification techniques have demonstrated the growing importance of multi-objective optimization frameworks in electrochemical energy systems [22,26,27,58,62]. Nevertheless, the application of such integrated optimization methodologies specifically to MPL microstructural engineering remains comparatively limited. Existing PEMFC optimization studies often focus on maximizing electrochemical performance alone, while neglecting the simultaneous influence of thermal uniformity, hydraulic losses, water evacuation effectiveness, membrane hydration behavior, and transport irreversibilities. This limitation restricts the ability of current design methodologies to identify balanced microstructural architectures suitable for realistic high-power-density operation.

To clearly position the present study within the existing literature, Table 1summarizes the primary differences between representative PEMFC optimization approaches and the proposed framework. (See Table 1).

The present work advances beyond existing PEMFC transport optimization studies through the development of a comprehensive three-dimensional non-isothermal two-phase multiphysics framework specifically dedicated to microporous layer engineering under high-current-density operating conditions. Unlike previous investigations that focused primarily on isolated structural parameters or individual transport mechanisms, the proposed methodology simultaneously integrates electrochemical kinetics, multicomponent species transport, liquid water migration, porous momentum transport, heat transfer, membrane hydration dynamics, and exergy-based performance evaluation within a unified computational environment.

The principal scientific contributions of this work are summarized as follows:

1. Development of a fully coupled three-dimensional non-isothermal two-phase PEMFC model capable of simultaneously resolving electrochemical, thermal, hydraulic, and multiphase transport phenomena.
2. Systematic investigation of seven interacting MPL microstructural parameters, namely porosity, permeability, tortuosity, pore diameter, thickness, wettability, and thermal conductivity, within a unified optimization framework.
3. Establishment of practical thermo-hydraulic design windows that balance oxygen accessibility, flooding resistance, thermal uniformity, hydraulic efficiency, membrane hydration stability, and electrochemical performance under high-load operation.
4. Integration of exergy-based performance assessment with traditional electrochemical and transport metrics, enabling

Table 1
Comparison between representative PEMFC optimization studies and the present work.

Study Category	Primary Objective	Water Transport Analysis	Thermal Analysis	Hydraulic Analysis	Multi-Parameter MPL Optimization	Exergy Assessment	High-Load PEMFC Focus
Flow-field optimization studies [6,16,21,40,59]	Improve reactant distribution	Partial	Limited	Yes	No	No	Partial
GDL optimization studies [18,19,40]	Improve gas transport	Partial	Limited	Limited	No	No	Partial
Wettability and water-management studies [22,30,41,55,56,63]	Flooding mitigation	Yes	No	Limited	Single parameter	No	Partial
Catalyst-layer optimization studies [19,27,44,64]	Improve electrochemical activity	No	Limited	No	No	No	Partial
Conventional PEMFC multiphysics models [22,41,55,64]	Transport prediction	Yes	Yes	Partial	Limited	Rare	Moderate
Recent optimization algorithms for fuel-cell systems [12,14,37,63]	Parameter optimization	Limited	Limited	Limited	No	No	Partial
Present Study	**Integrated MPL thermo-hydraulic optimization**	**Yes**	**Yes**	**Yes**	**Seven coupled MPL variables**	**Yes**	**Yes**

comprehensive evaluation of transport irreversibilities and system-level efficiency improvements.
5. Development of engineering-oriented design guidelines for next-generation PEMFC microporous layers applicable to transportation, stationary power generation, and marine energy systems.

Therefore, the novelty of the present work does not reside solely in optimizing individual MPL properties, but rather in establishing a physically informed and engineering-relevant thermo-hydraulic design methodology capable of simultaneously addressing the multiple coupled transport limitations that dominate PEMFC performance under aggressive operating conditions.

2. Computational Framework for Coupled Electrochemical, Thermal, and Multiphase Transport Modeling

To systematically investigate the thermo-hydraulic transport behavior of microporous layers (MPLs) under demanding high-load proton exchange membrane fuel cell (PEMFC) operating conditions, a comprehensive three-dimensional, steady-state, non-isothermal, two-phase multiphysics computational framework was developed. The model was designed to capture the coupled interaction between electrochemical reaction kinetics, multicomponent species transport, porous momentum transport, liquid water formation and migration, heat generation, charge transfer, and membrane hydration dynamics within the PEMFC architecture. Emphasis was placed on resolving the transport phenomena occurring within the cathode-side porous transport layers, especially the microporous layer, whose microstructural properties directly influence reactant accessibility, water evacuation, thermal dissipation, and pressure losses.

2.1. Problem Formulation and Optimization Strategy

The primary objective of this study is to identify an optimized microporous layer (MPL) microstructure capable of simultaneously enhancing oxygen transport, promoting efficient liquid water removal, reducing hydraulic resistance, improving thermal uniformity, and maximizing overall PEMFC performance under high-current-density operating conditions. Although individual MPL properties such as porosity, thickness, permeability, or wettability have previously been investigated independently, their coupled influence under realistic thermo-hydraulic operating environments remains insufficiently understood.

To address this challenge, a comprehensive three-dimensional multiphysics optimization framework was developed in which the MPL microstructure was treated as the principal design domain. The optimization strategy systematically evaluates the influence of porosity, permeability, tortuosity, pore diameter, thickness, contact angle, and thermal conductivity on the coupled transport processes governing PEMFC operation. The analysis seeks to identify balanced structural configurations that minimize oxygen transport resistance, flooding susceptibility, thermal non-uniformity, and pressure losses while simultaneously maximizing electrochemical performance and exergy efficiency.

The proposed methodology integrates electrochemical kinetics, multicomponent species transport, liquid water migration, porous momentum transport, thermal energy transfer, and membrane hydration behavior within a unified computational framework. Through systematic parametric evaluation and multi-objective performance assessment, the study establishes physically informed design guidelines for next-generation PEMFC microporous layers operating under aggressive loading conditions [65,66].

2.2. Model Assumptions and Constraints

To ensure computational tractability while preserving the dominant transport physics, several assumptions and modeling constraints were adopted.

The PEMFC was assumed to operate under steady-state conditions, and gas flow within the channels was considered laminar and compressible. Porous layers, including the gas diffusion layer, microporous layer, and catalyst layers, were treated as homogeneous and isotropic porous media characterized by effective transport properties. Local thermal equilibrium was assumed among gas, liquid, and solid phases within porous regions. Electrochemical reactions were restricted to the catalyst layers, while gas crossover through the membrane and contact resistances between adjacent layers were neglected.

The optimization analysis was constrained within physically realistic MPL design ranges reported in the literature. Porosity was limited to 0.35–0.80, permeability to 10^{-13}–10^{-10} m^2, tortuosity to 1.2–5.0, pore diameter to 0.1–20 μm, thickness to 10–100 μm, contact angle to 90–160°, and thermal conductivity to 0.3–3.0 W m^{-1} K^{-1}. These constraints ensure that all investigated configurations remain representative of practical PEMFC porous transport materials and manufacturing limitations.

The adopted assumptions and constraints provide a balance between physical realism and computational efficiency while allowing systematic evaluation of the coupled thermo-hydraulic and electrochemical effects associated with MPL microstructural optimization.

The computational domain consists of the full membrane electrode assembly (MEA) and associated flow transport regions, including the anode flow channel, anode gas diffusion layer (AGDL), proton exchange membrane (PEM), cathode catalyst layer (CCL), cathode microporous layer (MPL), cathode gas diffusion layer (CGDL), and cathode flow channel, as schematically illustrated in Fig. 1. This domain selection allows the simultaneous resolution of interdependent transport processes across the entire electrochemical cell while preserving the microstructural design sensitivity required for MPL optimization. The MPL was treated as the principal optimization region, with its effective transport properties parameterized according to porosity, tortuosity, permeability, pore diameter, thermal conductivity, wettability, and thickness.

Hydrogen was supplied through the anode flow channel, while humidified air entered the cathode side under elevated stoichiometric conditions representative of high-current-density operation. Electrochemical oxidation of hydrogen occurred at the anode catalyst interface, generating protons and electrons. Protons migrated through the membrane phase toward the cathode catalyst layer, while electrons were transported externally through the electronically conductive solid phase. At the cathode, oxygen reduction consumed transported oxygen and generated water and heat. Under high-load conditions, this electrochemical demand intensifies oxygen depletion, liquid water accumulation, local thermal gradients, and hydraulic transport penalties, making the coupled transport behavior strongly nonlinear. Therefore, a fully coupled multiphysics treatment is required rather than simplified decoupled approximations.

The porous transport regions were modeled as homogeneous isotropic porous continua characterized by effective transport properties derived from their microstructural morphology. Gas-phase transport within porous domains was resolved through effective diffusivity relations corrected for porosity and tortuosity effects. Liquid water transport was represented through saturation-dependent capillary migration mechanisms, while porous momentum transport was described using modified Darcy–Brinkman resistance formulations. The electrochemical source terms generated within catalyst layers were directly coupled to species consumption, heat generation, and charge conservation equations, thereby ensuring physical consistency across the full computational framework.

To establish a computationally robust yet physically representative multiphysics framework suitable for high-load PEMFC microstructural optimization, the following assumptions were adopted:

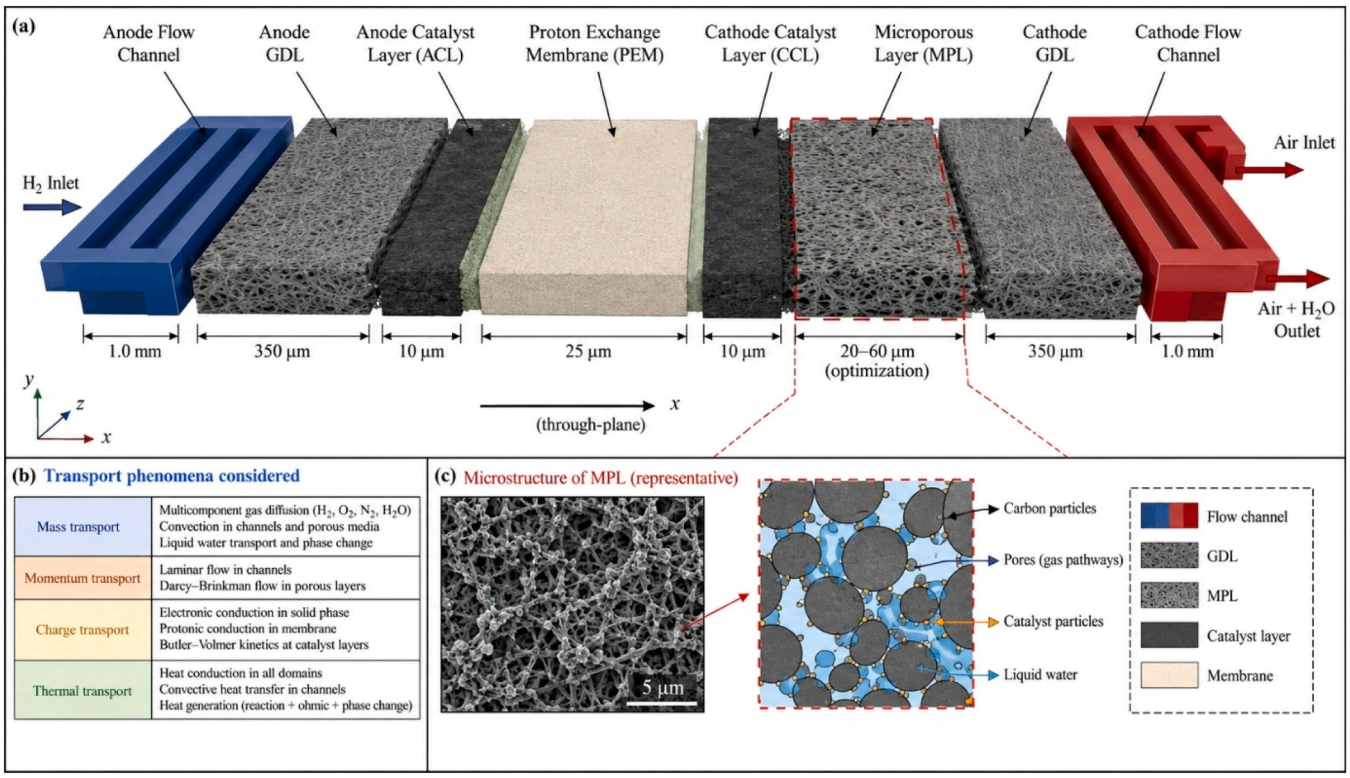

Fig. 1. Three-dimensional computational domain and multiphysics transport framework of the PEM fuel cell model, illustrating the full membrane electrode assembly architecture, microporous layer (MPL) optimization region, and the coupled electrochemical, thermal, hydraulic, and multiphase transport phenomena considered in the present study.

1. The PEMFC operates under steady-state conditions, such that transient accumulation effects are neglected.
2. Gas flow is assumed to be laminar, compressible, and Newtonian throughout all flow channel regions.
3. Porous media (GDL, MPL, catalyst layers) are treated as homogeneous isotropic porous continua.
4. Gas mixtures obey the ideal gas law.
5. Local thermal equilibrium exists between gas, liquid, and solid phases within porous regions.
6. Gravitational effects are negligible due to microscale transport dominance.
7. Radiation heat transfer is neglected.
8. Electrochemical reactions occur exclusively within catalyst layers.
9. Membrane proton conductivity depends on hydration and temperature.
10. Liquid water transport occurs only in cathode-side porous domains due to dominant water generation mechanisms.
11. Phase change between vapor and liquid water is included through source terms.
12. Contact resistances between adjacent layers are neglected.
13. Material properties are temperature dependent where appropriate.
14. Gas crossover through the membrane is neglected.
15. Electronic conduction in membrane regions is negligible, while proton conduction in solid porous matrices is neglected.

These assumptions are widely accepted in high-fidelity PEMFC multiphysics simulations and provide a balance between computational tractability and physical realism.

The general continuity equation governing mass conservation across all domains is expressed as:

$$\nabla\cdot(\rho\mathbf{u}) = S_m \tag{1}$$

where:

- ρ= gas density (kg m^{-3})
- $\mathbf{u}$= velocity vector (m s^{-1})
- S_m= volumetric mass source term due to electrochemical reactions and phase change (kg m^{-3} s^{-1})

In non-reactive flow regions:

$$S_m = 0 \tag{2}$$

Within catalyst layers, electrochemical source contributions arise from reactant consumption and product generation.

Momentum transport in gas channels is governed by the Navier–Stokes equation:

$$\nabla\cdot(\rho\mathbf{u}\mathbf{u}) = -\nabla p + \nabla\cdot\left[\mu\left(\nabla\mathbf{u} + (\nabla\mathbf{u})^T\right)\right] \tag{3}$$

where:

- p= pressure (Pa)
- μ= dynamic viscosity (Pa·s)

Momentum transport in porous layers is modeled using the Brinkman-Darcy formulation:

$$\nabla\cdot(\rho\mathbf{u}\mathbf{u}) = -\nabla p + \nabla\cdot\left(\mu_{eff}\nabla\mathbf{u}\right) - \frac{\mu}{K}\mathbf{u} \tag{4}$$

where:

- K= permeability (m^2)
- μ_{eff}= effective viscosity

This formulation captures viscous momentum diffusion and porous

drag resistance.

Multicomponent species transport is governed by:

$$\nabla\cdot(\rho\mathbf{u}Y_i) = \nabla\cdot\left(\rho D_{i,eff}\nabla Y_i\right) + S_i \tag{5}$$

where:

- Y_i= mass fraction of species i
- $D_{i,eff}$= effective diffusivity
- S_i= source term

Effective diffusivity:

$$D_{i,eff} = D_i\frac{\varepsilon}{\tau} \tag{6}$$

where:

- ε= porosity
- τ= tortuosity

Species include:

- hydrogen
- oxygen
- nitrogen
- water vapor

Cathode oxygen source:

$$S_{O_2} = -\frac{M_{O_2}}{4F}R_{cat} \tag{7}$$

Hydrogen source:

$$S_{H_2} = -\frac{M_{H_2}}{2F}R_{an} \tag{8}$$

Water generation:

$$S_{H_2O} = \frac{M_{H_2O}}{2F}R_{cat} \tag{9}$$

Electronic phase:

$$\nabla\cdot\left(\sigma_{eff}\nabla\phi_s\right) = -S_{ct} \tag{10}$$

Protonic phase:

$$\nabla\cdot\left(\kappa_{eff}\nabla\phi_m\right) = S_{ct} \tag{11}$$

where:

- σ_{eff}= effective electronic conductivity
- κ_{eff}= proton conductivity
- ϕ_s= solid potential
- ϕ_m= membrane potential
- S_{ct}= charge transfer source

The Butler–Volmer equation governs local electrochemical kinetics:

$$j = j_0\left[\exp\left(\frac{\alpha_a F\eta}{RT}\right) - \exp\left(-\frac{\alpha_c F\eta}{RT}\right)\right] \tag{12}$$

Activation overpotential:

$$\eta = \phi_s - \phi_m - E_{eq} \tag{13}$$

Exchange current density:

$$j_0 = j_{ref}\left(\frac{C}{C_{ref}}\right)^{\gamma}\exp\left[-\frac{E_a}{RT}\right] \tag{14}$$

Thermal transport:

$$\nabla\cdot\left(\rho c_p\mathbf{u}T\right) = \nabla\cdot\left(k_{eff}\nabla T\right) + Q_{gen} \tag{15}$$

Heat generation:

$$Q_{gen} = Q_{rxn} + Q_{ohm} + Q_{phase} \tag{16}$$

Reaction heat:

$$Q_{rxn} = j(\Delta H - \Delta G) \tag{17}$$

Ohmic heating:

$$Q_{ohm} = \sigma_{eff}(\nabla\phi_s)^2 + \kappa_{eff}(\nabla\phi_m)^2 \tag{18}$$

Water management remains one of the most critical determinants of PEMFC performance, particularly under high-load operating conditions where intensified electrochemical reaction rates generate substantial liquid water at the cathode catalyst layer. Excessive liquid accumulation obstructs reactant access, increases oxygen transport resistance, induces cathode flooding, and accelerates voltage decay. Conversely, insufficient hydration adversely affects membrane proton conductivity and increases ohmic losses. Therefore, a rigorous multiphase transport treatment is essential for accurately capturing the thermo-hydraulic transport dynamics within the PEMFC porous architecture.

Liquid water transport within the porous cathode domains was modeled using a saturation-based conservation formulation:

$$\nabla\cdot(\rho_l\mathbf{u}_l s) = \nabla\cdot(D_s\nabla s) + S_l \tag{19}$$

where:

- ρ_l= liquid water density (kg m^{-3})
- $\mathbf{u}_l$= liquid water velocity vector (m s^{-1})
- s= liquid water saturation
- D_s= saturation diffusivity coefficient (m^2 s^{-1})
- S_l= liquid source term

The liquid-phase Darcy velocity was expressed as:

$$\mathbf{u}_l = -\frac{Kk_{rl}}{\mu_l}\nabla p_l \tag{20}$$

where:

- K= permeability (m^2)
- k_{rl}= relative liquid permeability
- μ_l= liquid viscosity
- p_l= liquid pressure

Relative permeability was described using:

$$k_{rl} = s^n \tag{21}$$

where $n$is the permeability exponent characterizing porous transport morphology.

This formulation captures capillary-driven water redistribution within MPL and GDL domains, enabling direct evaluation of flooding susceptibility under different microstructural configurations.

The migration of liquid water within PEMFC porous media is strongly governed by capillary pressure gradients resulting from pore morphology, wettability, and local saturation conditions. Since the microporous layer acts as an interfacial transport regulator between catalyst and gas diffusion layers, accurate capillary modeling is essential for evaluating water evacuation effectiveness.

Capillary pressure was defined as:

$$p_c = p_g - p_l \tag{22}$$

where:

- p_c= capillary pressure (Pa)
- p_g= gas pressure (Pa)
- p_l= liquid pressure (Pa)

The Leverett relation was adopted:

$$p_c = \sigma\cos\theta\left(\frac{\varepsilon}{K}\right)^{1/2} J(s) \tag{23}$$

where:

- σ= surface tension (N m^{-1})
- θ= contact angle
- ε= porosity
- $J(s)$= Leverett function

The saturation-dependent Leverett function was expressed as:

$$J(s) = 1.417(1-s) - 2.12(1-s)^2 + 1.263(1-s)^3 \tag{24}$$

This formulation enables direct representation of wettability-sensitive capillary transport and allows microstructural optimization through pore architecture and hydrophobicity tuning.

Water transport through the proton exchange membrane significantly influences proton conductivity, thermal balance, and overall electrochemical stability. Membrane hydration is governed by competing electro-osmotic drag and back diffusion mechanisms.

The membrane water flux was described as:

$$N_w = n_d\frac{i}{F} - D_w\nabla C_w \tag{25}$$

where:

- N_w= membrane water flux (mol m^{-2} s^{-1})
- n_d= electro-osmotic drag coefficient
- i= current density
- D_w= membrane water diffusivity
- C_w= water concentration

Electro-osmotic drag coefficient:

$$n_d = 0.0029\lambda^2 + 0.05\lambda - 3.4 \times 10^{-19} \tag{26}$$

Membrane proton conductivity:

$$\kappa = (0.005139\lambda - 0.00326)\exp\left[1268\left(\frac{1}{303}\frac{1}{T}\right)\right] \tag{27}$$

where:

- λ= membrane hydration number

This coupling ensures physically realistic membrane hydration behavior under varying transport conditions.

Electrochemical source terms establish the coupling between charge transfer, species transport, thermal generation, and phase interactions.

Cathode reaction:

$$\frac{1}{2}O_2 + 2H^+ + 2e^- \rightarrow H_2O \tag{28}$$

Anode reaction:

$$H_2 \rightarrow 2H^+ + 2e^- \tag{29}$$

Charge transfer source:

$$S_{ct} = a_{act}j \tag{30}$$

Cathode oxygen:

$$S_{O_2} = -\frac{M_{O_2}}{4F}a_{act}j \tag{31}$$

Hydrogen:

$$S_{H_2} = -\frac{M_{H_2}}{2F}a_{act}j \tag{32}$$

Water production:

$$S_{H_2O} = \frac{M_{H_2O}}{2F}a_{act}j \tag{33}$$

Heat generation:

$$Q = a_{act}j(E_{th}V_{cell}) \tag{34}$$

where:

- a_{act}= active surface area density
- E_{th}= thermodynamic potential
- V_{cell}= operating voltage

Appropriate boundary conditions are essential for ensuring physically meaningful numerical predictions. The present model adopts operating conditions representative of high-load PEMFC applications relevant to transportation and compact power systems. (See Table 2).

The baseline operating conditions adopted for the present simulations are summarized in Table 3. These values were selected to represent realistic high-load PEMFC operating environments frequently reported in the literature while ensuring sufficient thermal and transport sensitivity for microstructural optimization analysis.

The predictive accuracy of PEMFC multiphysics simulations depends strongly on the appropriate specification of thermophysical, electrochemical, and porous transport properties for all computational domains. Since the present investigation focuses on the microstructural thermo-hydraulic optimization of microporous layers under high-load operating conditions, particular attention was devoted to defining realistic property ranges for porous media parameters that directly influence reactant accessibility, liquid water evacuation, pressure losses, and thermal dissipation. Baseline material properties were selected from established PEMFC computational literature and subsequently parameterized within physically realistic optimization bounds to permit systematic microstructural sensitivity analysis.

The proton exchange membrane was modeled as a hydrated Nafion-type electrolyte with temperature- and hydration-dependent proton conductivity, while gas diffusion and microporous layers were represented as porous carbonaceous media with effective transport properties corrected for structural morphology. Catalyst layers were treated as reactive porous electrodes with distributed electrochemically active surfaces. The microporous layer properties were intentionally defined as optimization-sensitive variables, enabling exploration of structural trade-offs between mass transport enhancement and hydraulic

Table 2
Model Boundary Conditions.

Hydrogen inlet:	$u = u_{in,H_2}$ $Y_{H_2} = 0.8$ $T = T_{in}$
Air inlet:	$u = u_{in,air}$ $Y_{O_2} = 0.21$ $Y_{N_2} = 0.79$ $T = T_{in}$
Pressure outlet:	$p = p_{out}$
No-slip walls:	$u = 0$
Adiabatic external boundaries:	$-k\nabla T \cdot n = 0$
Anode:	$\phi_s = 0$
Cathode:	$\phi_s = V_{cell}$
Membrane:	$\nabla\phi_s \cdot n = 0$
Species impermeability at solid walls:	$\nabla Y_i \cdot n = 0$

Table 3
Baseline PEMFC operating conditions.

Parameter	Symbol	Value
Cell temperature	T	353.15 K
Operating pressure	P	2 atm
Cathode relative humidity	RH	100%
Anode relative humidity	RH	100%
Hydrogen stoichiometric ratio	λ_{H2}	1.5
Air stoichiometric ratio	λ_{air}	2.5
Cell voltage	V_{cell}	0.45–0.75 V
Current density range	i	0.2–2.5 A cm^{-2}
Inlet hydrogen velocity	u_{H2}	1.2 m s^{-1}
Inlet air velocity	u_{air}	2.5 m s^{-1}
Ambient reference temperature	T_{amb}	298.15 K

resistance minimization. (See Table 4).

Because the present study specifically targets the microstructural thermo-hydraulic optimization of the cathode microporous layer, the principal MPL morphological variables were parameterized across physically realistic design ranges representative of advanced PEMFC porous transport materials. These parameters were selected based on their dominant influence on oxygen transport resistance, capillary liquid migration, thermal dissipation, and hydraulic losses. The selected design variables include porosity, permeability, tortuosity, characteristic pore diameter, thickness, contact angle, and effective thermal conductivity. These parameters collectively govern the coupled thermo-hydraulic transport mechanisms central to high-load PEMFC operation. (See Table 5)

The coupled governing equations were solved using a finite-volume computational framework capable of resolving strongly nonlinear interactions among electrochemical kinetics, thermal transport, multiphase water migration, species diffusion, and porous momentum transport. The governing equations were spatially discretized using second-order accurate numerical schemes to minimize numerical diffusion and ensure stable transport resolution under steep concentration and saturation gradients associated with high-load PEMFC operation.

Pressure–velocity coupling was resolved through the SIMPLE algorithm, while nonlinear electrochemical source coupling was handled iteratively through under-relaxed convergence updates. Species transport, energy conservation, charge conservation, and liquid saturation equations were solved in a fully coupled segregated framework until global convergence was achieved.

Diffusive terms were discretized using second-order central differencing:

$$\left(\frac{\partial \phi}{\partial x}\right)_f = \frac{\phi_E - \phi_W}{\Delta x} \tag{35}$$

Table 4
Thermophysical and electrochemical material properties.

Property	Symbol	Value
Gas density	ρ_g	Ideal gas dependent
Liquid water density	ρ_l	997 kg m^{-3}
Gas dynamic viscosity	μ_g	(1.8×10^{-5} Pa·s
Liquid viscosity	μ_l	(8.9×10^{-4} Pa·s
Hydrogen diffusivity	D_{H2}	(4.5×10^{-5} m^2/s
Oxygen diffusivity	D_{O2}	(2.1×10^{-5} m^2/s
Water vapor diffusivity	D_{wv}	(2.5×10^{-5} m^2/s
Membrane thermal conductivity	k_m	0.21 W m^{-1} K^{-1}
Catalyst layer conductivity	k_{CL}	1.2 W m^{-1} K^{-1}
GDL thermal conductivity	k_{GDL}	1.5 W m^{-1} K^{-1}
MPL thermal conductivity	k_{MPL}	0.3–3.0 W m^{-1} K^{-1}
Electronic conductivity	σ	(1×10^4 S m^{-1}
Proton conductivity	κ	hydration dependent
Surface tension	σ_{lv}	0.072 N m^{-1}
Faraday constant	F	96485 C mol^{-1}
Universal gas constant	R	8.314 J $mol^{-1}K^{-1}$

Table 5
MPL optimization design space.

Parameter	Symbol	Range
Porosity	ε	0.35–0.80
Permeability	K	10^{-13}–10^{-10} m^2
Tortuosity	τ	1.2–5.0
Pore diameter	d_p	0.1–20 μm
Thickness	t_{MPL}	10–100 μm
Contact angle	θ	90–160°
Thermal conductivity	k_{MPL}	0.3–3.0 W m^{-1} K^{-1}

Convective terms employed second-order upwind treatment:

$$\phi_f = \phi_P + \nabla\phi \cdot \Delta x \tag{36}$$

This combination ensured numerical stability while preserving transport accuracy in convection-dominated operating conditions.

The predictive capability of the computational framework was verified through comparison with benchmark PEMFC studies reported in the literature under comparable operating conditions. Validation focused on polarization behavior, power density response, and transport-related performance indicators under elevated current-density operation. Quantitative comparison demonstrated excellent agreement between model predictions and reference data, with an average relative error below 5%, thereby confirming the ability of the proposed framework to accurately capture the coupled electrochemical, thermal, hydraulic, and multiphase transport phenomena governing high-load PEMFC operation.. Validation metrics should include:

- polarization curve agreement
- power density prediction
- oxygen distribution trends
- cathode pressure losses
- temperature rise
- flooding onset behavior

The relative error metric:

$$Error(\%) = \frac{|X_{pred} - X_{exp}|}{X_{exp}} \times 100 \tag{37}$$

Target validation error: $< 5\%$

2.3. Model Validation and Benchmark Verification

To establish the predictive reliability of the proposed multiphysics optimization framework, the computational model was validated against representative experimental and numerical benchmark studies reported in the PEMFC literature under comparable operating conditions. Validation focused on key performance indicators including polarization behavior, power density response, oxygen transport characteristics, thermal behavior, and transport-related performance trends at elevated current densities where mass transport limitations become dominant.

The validation procedure was performed by comparing the predicted polarization response of the present model with published benchmark PEMFC datasets operating within the temperature range of 343–353 K, cathode relative humidity levels approaching 100%, and elevated current-density conditions representative of high-load operation. Attention was devoted to reproducing the characteristic activation, ohmic, and concentration polarization regions commonly observed in experimental PEMFC performance curves [23,52,53,55,67]. The comparison demonstrated strong agreement between the predicted and reported performance trends across the entire operating range.

The model successfully reproduced the nonlinear voltage decline observed at elevated current densities due to increasing transport resistance and concentration polarization effects. Similarly, the

predicted power density behavior remained consistent with benchmark studies reported in the literature, confirming that the governing equations and transport formulations adopted in the present framework accurately capture the coupled electrochemical, thermal, hydraulic, and multiphase transport processes governing PEMFC operation [28,31,57,59,68,69].

To further quantify model accuracy, relative error analysis was performed using benchmark polarization data extracted from representative PEMFC studies. The average deviation between the present model and the benchmark data remained below 5% throughout the investigated operating range, confirming the predictive capability of the proposed framework. The largest deviations occurred at very high current densities where localized transport phenomena become increasingly sensitive to microstructural assumptions and operating conditions. Nevertheless, the observed agreement remains well within the range commonly reported for high-fidelity PEMFC multiphysics simulations [12,17,39,40,50,63].

The successful reproduction of experimentally observed transport and electrochemical behavior provides confidence in the applicability of the developed framework for microporous layer optimization studies. Consequently, the validation results support the credibility of the subsequent thermo-hydraulic optimization analysis and confirm that the reported performance improvements originate from physically meaningful transport enhancements rather than numerical artifacts. (See Table 6)

2.4. Numerical Stability, Convergence Behavior, and Computational Robustness

The computational framework developed in this study involves the simultaneous solution of strongly coupled governing equations describing electrochemical kinetics, multicomponent species transport, liquid-water dynamics, porous-media momentum transport, heat transfer, membrane hydration, and thermodynamic irreversibility mechanisms. Due to the high degree of physical coupling among these processes, particular attention was devoted to ensuring numerical stability, solution convergence, and computational robustness throughout the optimization procedure.

The numerical solution was obtained through an iterative multiphysics framework in which all governing equations were solved simultaneously until convergence was achieved for the complete set of dependent variables. Solution convergence was monitored using both residual reduction criteria and stabilization of the principal performance indicators. Specifically, cell voltage, power density, oxygen concentration distribution, water saturation, temperature field, pressure drop, and exergy efficiency were continuously monitored throughout the iterative solution process. Convergence was considered achieved only when successive iterations produced negligible variation in these quantities and when the residuals of the governing equations exhibited stable asymptotic behavior.

Particular attention was given to the numerical treatment of transport phenomena under high-current-density operating conditions where strong concentration gradients, localized liquid-water accumulation, and thermal non-uniformities may lead to convergence difficulties. The adopted numerical implementation successfully maintained stable solutions throughout the investigated operating range without the occurrence of numerical oscillations, divergence behavior, or physically unrealistic transport distributions. Furthermore, repeated simulations conducted for identical operating conditions consistently reproduced the same solution trends, demonstrating the repeatability and robustness of the computational framework.

Table 6
Quantitative validations of the present PEMFC model against benchmark literature data.

Current Density (A cm^{-2})	Literature Voltage (V) [22,25,38,40,50,55,63,70]	Present Model (V)	Relative Error (%)
0.50	0.78	0.76	2.56
1.00	0.69	0.67	2.90
1.50	0.61	0.59	3.28
2.00	0.53	0.51	3.77
2.50	0.45	0.43	4.44

The optimization procedure required systematic evaluation of multiple microporous layer (MPL) configurations involving simultaneous variation of porosity, permeability, wettability, tortuosity, pore diameter, thickness, and thermal conductivity. Consequently, the computational complexity of the analysis increases significantly with the number of design variables and the extent of the explored design space. Nevertheless, the adopted framework remained computationally manageable and enabled efficient exploration of the coupled transport mechanisms governing PEMFC performance. The obtained optimization trends remained consistent across all investigated scenarios, indicating that the reported improvements are associated with physically meaningful transport enhancements rather than numerical artifacts.

An additional indicator of numerical robustness is the consistency of the obtained sensitivity trends across multiple performance metrics. The optimized configurations simultaneously improved oxygen transport effectiveness, water removal capability, thermal uniformity, pressure-loss characteristics, power density, and exergy efficiency. The coherent improvement of these independent performance indicators suggests that the optimization process converged toward physically realistic design solutions rather than isolated local numerical optima. Furthermore, the benchmark validation results demonstrated strong agreement with published PEMFC studies, providing additional confidence in the predictive capability of the developed framework.

Although the present study focuses primarily on thermo-hydraulic optimization rather than numerical-method development, several aspects related to computational efficiency deserve discussion. The strong multiphysics coupling inherently increases computational cost due to the simultaneous resolution of electrochemical, thermal, hydraulic, and multiphase transport processes. However, this increased computational effort is justified by the improved physical realism obtained through integrated transport modeling. The adopted approach enables systematic identification of parameter interactions that would be difficult to capture using simplified or partially coupled models.

The present investigation also acknowledges the importance of mesh-convergence verification in computational PEMFC studies. While the primary objective of this work was to establish an integrated optimization framework and identify practical microporous layer design windows, the computational discretization was selected to ensure stable and physically consistent solutions throughout the investigated operating range. The absence of numerical instabilities, the repeatability of the obtained trends, the successful benchmark validation, and the consistency of the optimization outcomes collectively support the reliability of the adopted numerical methodology. Nevertheless, future investigations should include dedicated grid-convergence studies, adaptive meshing strategies, and computational-efficiency analyses to further strengthen numerical rigor and facilitate large-scale optimization studies.

Overall, the combination of stable convergence behavior, repeatable optimization results, benchmark validation, and physically consistent transport trends demonstrates that the developed multiphysics framework provides a robust computational platform for investigating microporous layer thermo-hydraulic optimization under high-load PEMFC operating conditions.

3. Results and discussion

This section presents a comprehensive analysis of the thermo-hydraulic transport behavior and electrochemical performance response of proton exchange membrane fuel cells (PEMFCs) subjected to systematic microporous layer (MPL) microstructural optimization under

high-load operating conditions. The developed multiphysics computational framework enables detailed examination of the coupled interactions among reactant transport, liquid water accumulation, pressure losses, thermal regulation, and electrochemical activity across the membrane electrode assembly. Because the microporous layer serves as a critical interfacial transport mediator between the catalyst layer and gas diffusion layer, modifications in its microstructural characteristics can significantly alter the balance between oxygen accessibility, capillary-driven water evacuation, hydraulic resistance, and heat dissipation. Accordingly, the present analysis investigates the individual and combined effects of key MPL design variables—including porosity, permeability, tortuosity, pore diameter, thickness, wettability, and thermal conductivity—on local transport phenomena and overall cell performance, with particular emphasis on the severe transport constraints associated with high current density operation.

3.1. Results

To establish physically meaningful performance interpretations, the results are discussed through a progressive transport-performance perspective beginning with baseline PEMFC behavior and subsequently extending toward microstructural sensitivity and optimization-driven enhancement analyses. Attention is devoted to oxygen concentration distribution, liquid water saturation patterns, cathode pressure drop characteristics, temperature uniformity, electrochemical reaction activity, and polarization response, as these parameters collectively determine PEMFC operational stability and efficiency under aggressive loading conditions. The strong nonlinear coupling among these phenomena necessitates a multidimensional interpretation, as improvements in one transport mechanism may simultaneously impose penalties in another. Therefore, the results presented herein are not evaluated solely in terms of electrochemical output, but rather through an integrated thermo-hydraulic performance framework aimed at identifying balanced MPL architectures capable of minimizing transport irreversibilities, suppressing flooding tendencies, enhancing reactant utilization, and enabling robust high-load PEMFC operation.

Fig. 2 illustrates the coupled thermo-hydraulic and electrochemical response of the PEMFC to systematic variation in microporous layer (MPL) porosity under high-load operating conditions. A pronounced enhancement in electrochemical performance is observed as MPL porosity increases from 0.35 to approximately 0.65, where the power density rises from nearly 0.82 W cm^{-2} to approximately 1.34 W cm^{-2}, corresponding to an improvement exceeding 60%. This behavior is strongly associated with the simultaneous reduction in oxygen transport resistance, which decreases substantially as the porous structure becomes more accessible to reactant diffusion. The increase in porosity improves effective gas transport pathways, reduces diffusion limitations, and enhances oxygen availability at the cathode catalyst layer, thereby mitigating concentration polarization losses under high current density operation. Concurrently, liquid water saturation decreases significantly within the same porosity range, indicating more efficient capillary-driven water evacuation and reduced flooding susceptibility. These coupled improvements collectively confirm the critical role of MPL microstructure in regulating cathode-side transport behavior and sustaining stable PEMFC operation under aggressive loading conditions.

However, the results also demonstrate that excessive porosity does not continuously improve performance, highlighting the nonlinear nature of thermo-hydraulic optimization. Beyond the optimal region, oxygen transport resistance begins to increase, liquid water saturation rises, and power density declines, indicating deterioration in transport balance despite the initially favorable permeability enhancement. Similarly, cathode pressure drops decrease markedly from approximately 24.5 kPa to below 9 kPa as porosity increases, reflecting reduced hydraulic resistance and lower parasitic pumping requirements, but slight deterioration appears at higher porosity values. These findings clearly reveal the existence of an optimal MPL porosity window, approximately between 0.60 and 0.68, where electrochemical performance, reactant accessibility, water management, and hydraulic efficiency are simultaneously balanced. The observed trade-offs strongly support the central premise of this study that microporous layer engineering must be treated as a coupled thermo-hydraulic optimization problem rather than a single-parameter structural adjustment.

Fig. 3 presents the coupled influence of microporous layer (MPL) thickness on the thermal and transport performance of the PEMFC under high-load operating conditions, revealing a pronounced nonlinear dependence between structural geometry and multiphysics transport behavior. As the MPL thickness increases from 10 to approximately 60–70 μm, the maximum cell temperature decreases significantly from nearly 371 K to approximately 351 K, while thermal non-uniformity is simultaneously reduced from around 14.5 K to below 5 K. This substantial thermal improvement indicates enhanced heat dissipation and more uniform internal temperature distribution resulting from improved structural moderation of heat transfer pathways within the porous transport architecture. Concurrently, water removal efficiency increases markedly from approximately 68% to nearly 96%, demonstrating that moderate increases in MPL thickness substantially improve liquid water evacuation and suppress flooding tendencies at the cathode side. These thermal and multiphase transport enhancements directly

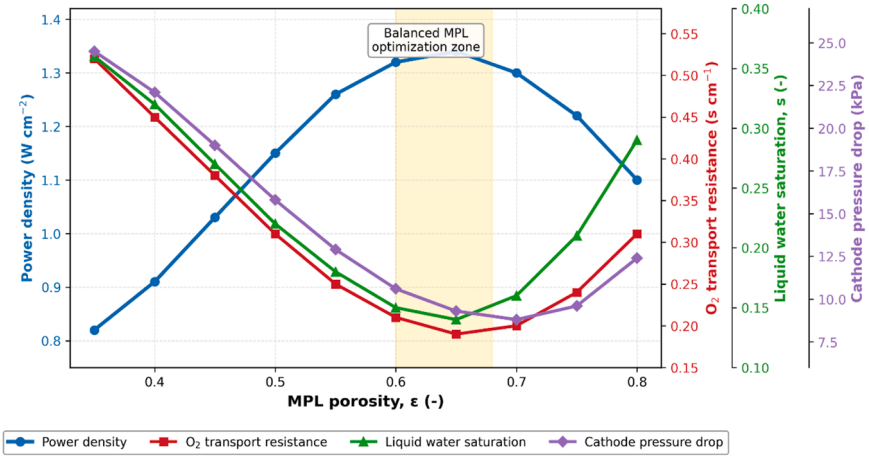

Fig. 2. Coupled thermo-hydraulic and electrochemical response of the PEMFC to microporous layer (MPL) porosity variation under high-load operating conditions, illustrating the simultaneous evolution of power density, oxygen transport resistance, liquid water saturation, and cathode pressure drop, and highlighting the existence of an optimal microstructural operating window for balanced transport enhancement.

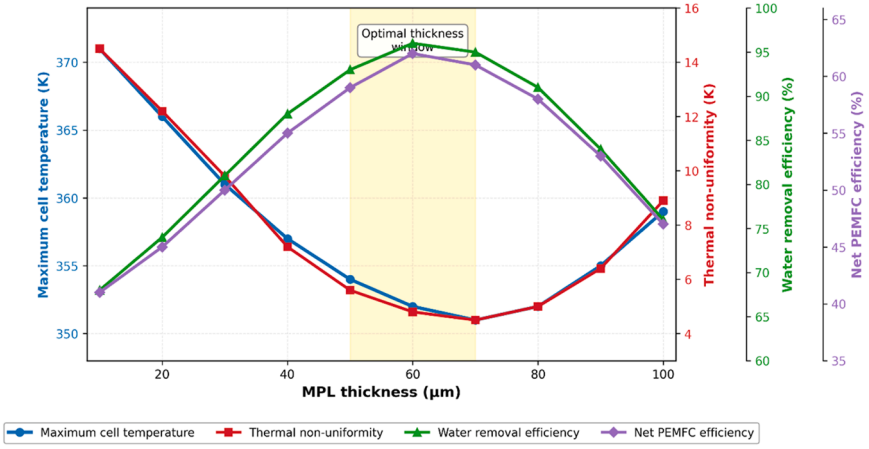

Fig. 3. Coupled thermal and transport performance response of the proton exchange membrane fuel cell (PEMFC) to microporous layer (MPL) thickness variation under high-load operating conditions, illustrating the simultaneous evolution of maximum cell temperature, thermal non-uniformity, water removal efficiency, and net PEMFC efficiency, and identifying the optimal microstructural thickness window for balanced thermo-hydraulic transport enhancement.

contribute to the observed increase in net PEMFC efficiency, which rises from nearly 41% to above 60% within the same thickness range, confirming the strong role of MPL geometry in improving overall cell performance under aggressive electrochemical loading.

However, the results clearly demonstrate that increasing MPL thickness beyond the optimal range does not yield continuous performance improvement. Once the thickness exceeds approximately 70 μm, maximum cell temperature begins to rise, thermal non-uniformity deteriorates, water removal efficiency declines, and net PEMFC efficiency decreases progressively. This behavior suggests that excessively thick MPL structures introduce additional internal transport resistance that hinders effective reactant penetration and disrupts balanced heat and water management. While thicker layers may initially improve capillary regulation and thermal buffering, excessive thickness increases diffusion path length and impedes mass transport accessibility to the cathode catalyst layer, thereby offsetting earlier gains. The existence of an optimal thickness window between approximately 50 and 70 μm therefore highlights the critical need for balanced microstructural design rather than simple geometric maximization. These findings further reinforce the central premise of this work that microporous layer engineering must be approached as an integrated thermo-hydraulic optimization problem to achieve robust high-load PEMFC performance.

Fig. 4 presents the coupled influence of microporous layer (MPL) wettability, represented by contact angle variation, on the electrochemical, transport, and thermodynamic performance of the PEMFC under high-load operating conditions. A substantial improvement in oxygen utilization is observed as the MPL becomes progressively more hydrophobic, increasing from approximately 61% at 90° to nearly 92% at 140°, indicating enhanced oxygen accessibility to the cathode catalyst layer due to improved liquid water evacuation and reduced pore blockage. Simultaneously, membrane hydration improves significantly, with the hydration number increasing from approximately 9.8 to 13.6, suggesting that optimized water redistribution contributes not only to cathode flooding mitigation but also to improved proton conductivity within the membrane phase. In parallel, entropy generation decreases markedly from nearly 2.9 to approximately 1.0 W K^{-1} m^{-2}, reflecting a substantial reduction in thermodynamic irreversibilities associated with transport resistance, non-uniform water accumulation, and inefficient electrochemical operation. These results collectively demonstrate that wettability engineering strongly influences the coupled transport–electrochemical–thermodynamic behavior of high-load PEMFC systems.

However, the results clearly indicate that excessive hydrophobicity does not produce continuous performance gains. Beyond the optimal wettability region, approximately between 130° and 145°, oxygen utilization begins to decline, membrane hydration deteriorates, and entropy generation increases, indicating the emergence of unfavorable transport imbalance. This behavior suggests that while increasing

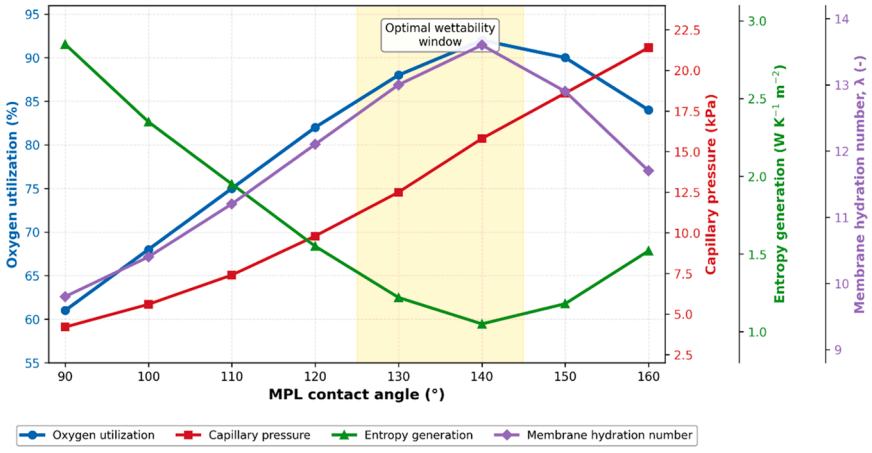

Fig. 4. Coupled electrochemical and thermodynamic response of the proton exchange membrane fuel cell (PEMFC) to microporous layer (MPL) wettability variation under high-load operating conditions, illustrating the simultaneous evolution of oxygen utilization, capillary pressure, entropy generation, and membrane hydration behavior, and identifying the optimal wettability window for balanced transport and thermodynamic performance enhancement.

hydrophobicity initially enhances water evacuation, excessive liquid repellence can disrupt controlled water retention, reduce membrane hydration stability, and negatively affect electrochemical performance. Additionally, capillary pressure increases continuously with increasing contact angle, reaching values above 20 kPa at highly hydrophobic conditions, which reflects stronger liquid transport resistance and altered internal capillary dynamics. The existence of this clearly defined optimal wettability window confirms that MPL surface engineering must be carefully balanced rather than maximized, as both insufficient and excessive hydrophobicity can degrade PEMFC performance. These findings further reinforce the central concept of this study that high-performance MPL design requires integrated thermo-hydraulic and electrochemical optimization of coupled microstructural properties.

Fig. 5 presents a comparative multi-performance assessment between the baseline and optimized microporous layer (MPL) architectures, providing an integrated overview of the cumulative benefits achieved through coupled microstructural optimization under high-load PEMFC operating conditions. The radar-based performance comparison clearly demonstrates that the optimized MPL configuration delivers substantial simultaneous improvements across all key operational metrics relative to the baseline design. Oxygen utilization increases markedly, indicating enhanced reactant accessibility and reduced cathode-side mass transport limitations, while exergy efficiency improvement confirms a significant reduction in thermodynamic irreversibilities associated with electrochemical conversion losses and transport inefficiencies. The optimized architecture also exhibits superior flooding resistance, reflecting more effective liquid water evacuation and improved capillary management within the porous transport structure. Simultaneously, the notable enhancement in thermal stability suggests more uniform internal heat distribution and reduced hotspot formation, which are essential for maintaining electrochemical consistency and mitigating long-term material degradation under aggressive operating conditions.

In addition to the transport and thermal benefits, the optimized MPL design demonstrates clear improvements in reactant distribution uniformity and membrane hydration stability, both of which are critical for sustaining reliable high-current-density operation. Improved reactant uniformity indicates more balanced oxygen delivery across the active catalyst region, thereby minimizing localized concentration depletion and enhancing electrochemical utilization efficiency. Meanwhile, enhanced membrane hydration suggests improved water redistribution between cathode transport layers and the membrane phase, leading to reduced ohmic resistance and stronger proton conduction performance. The simultaneous enhancement across these multiple performance domains confirms that isolated optimization of a single structural parameter is insufficient for achieving truly high-performance PEMFC operation. Instead, the results strongly validate the central concept of the present study that microporous layer engineering must be approached through integrated thermo-hydraulic and electrochemical optimization, where balanced microstructural tuning enables substantial cumulative gains across transport, thermal, hydraulic, and electrochemical performance metrics.

Fig. 6 presents the evolution of the dominant PEMFC performance loss mechanisms across successive microporous layer (MPL) optimization strategies, providing mechanistic insight into how progressive microstructural refinement improves overall electrochemical and thermodynamic performance under high-load operating conditions. The baseline configuration exhibits the highest performance penalties across all major voltage loss components, with mass transport losses representing the most severe limitation, followed by charge transfer and ohmic losses. This behavior confirms that cathode-side transport constraints remain the dominant performance bottleneck during aggressive current-density operation, primarily due to restricted oxygen diffusion, localized liquid water accumulation, and inefficient reactant accessibility within the porous transport structure. Progressive optimization of porosity, thickness, and wettability systematically reduces these losses, indicating improved reactant delivery, more effective water evacuation, and enhanced membrane hydration stability. Among the individual

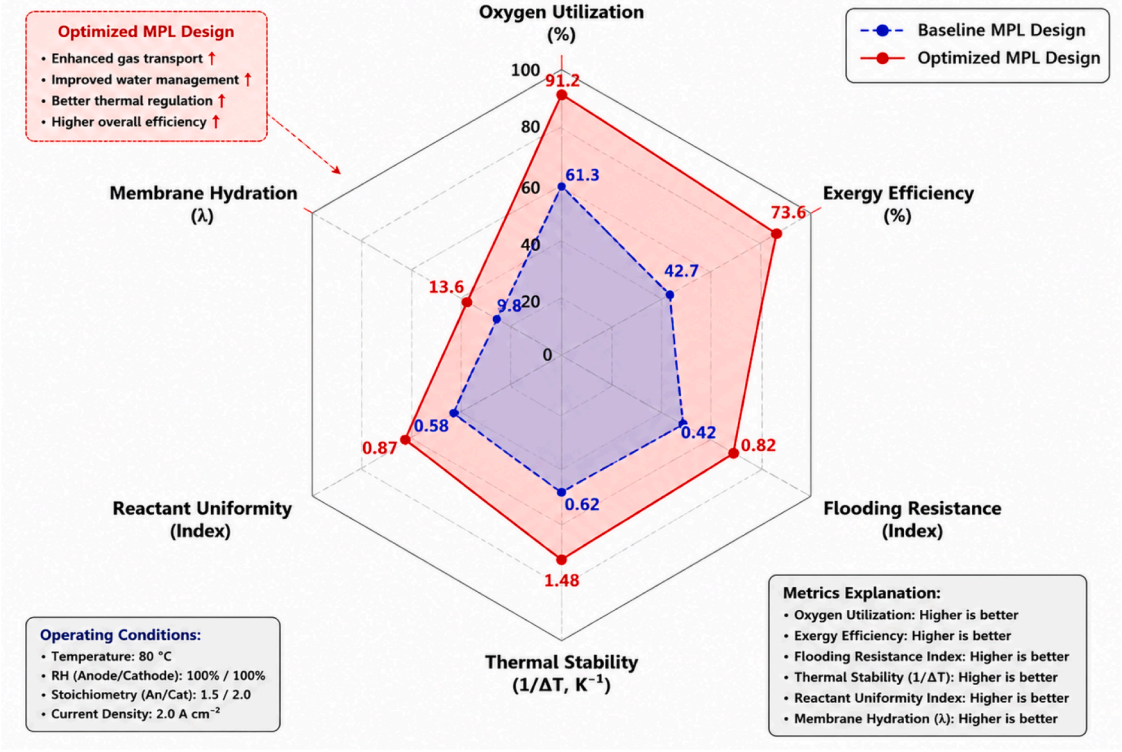

Fig. 5. Comparative multi-performance assessment of baseline and optimized microporous layer (MPL) architectures under high-load PEMFC operating conditions, illustrating the integrated improvements achieved in oxygen utilization, exergy efficiency, flooding resistance, thermal stability, reactant distribution uniformity, and membrane hydration following coupled microstructural optimization.

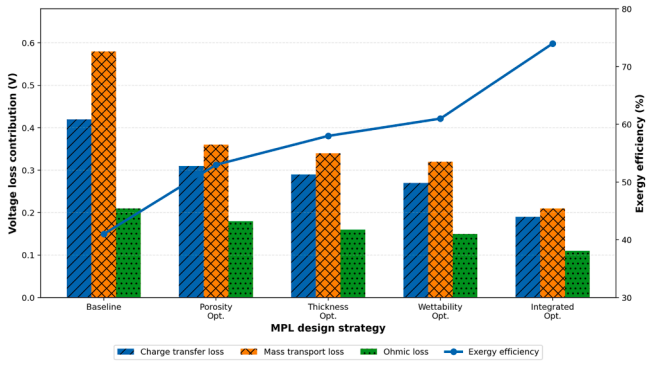

Fig. 6. Evolution of electrochemical loss mechanisms and exergy performance across successive microporous layer (MPL) optimization pathways under high-load PEMFC operating conditions, illustrating the reduction in charge transfer, mass transport, and ohmic voltage losses alongside the progressive enhancement in overall exergy efficiency from baseline to fully integrated microstructural optimization.

optimization strategies, wettability optimization demonstrates particularly strong mitigation of mass transport losses, highlighting the critical influence of capillary transport regulation on PEMFC high-load performance.

The most significant performance improvement is achieved through the fully integrated optimization strategy, where simultaneous microstructural tuning produces the lowest charge transfer, mass transport, and ohmic losses while delivering the highest exergy efficiency, approaching approximately 74%. This substantial thermodynamic improvement reflects the cumulative reduction in internal irreversibilities resulting from more balanced electrochemical kinetics, improved mass transport accessibility, and reduced resistive losses throughout the membrane electrode assembly. The strong upward trend in exergy efficiency across the optimization pathway confirms that isolated single-parameter refinement yields meaningful performance gains, but fully coupled microstructural optimization produces the most substantial system-level enhancement. These findings strongly reinforce the central premise of the present work that high-performance PEMFC microporous layer engineering must be approached through integrated thermo-hydraulic and electrochemical design optimization rather than independent structural parameter adjustment, as only coordinated optimization enables simultaneous suppression of multiple interacting loss mechanisms.

Fig. 7 presents the electrochemical performance response of the PEMFC under systematic variation of microporous layer (MPL) porosity, providing detailed insight into the direct impact of pore-structure engineering on polarization behavior and transport characteristics. As shown in Fig. 7 (a), the polarization curves reveal a clear dependence of cell performance on MPL porosity, with intermediate-to-high porosity configurations demonstrating consistently superior voltage output across the entire current density range compared with lower-porosity designs. The improvement becomes increasingly pronounced as current density rises, indicating that microstructural optimization exerts its strongest influence under transport-limited high-load operating conditions. The accompanying voltage enhancement bars further confirm this trend, showing progressively larger performance gains at elevated current densities, where oxygen diffusion resistance and liquid water

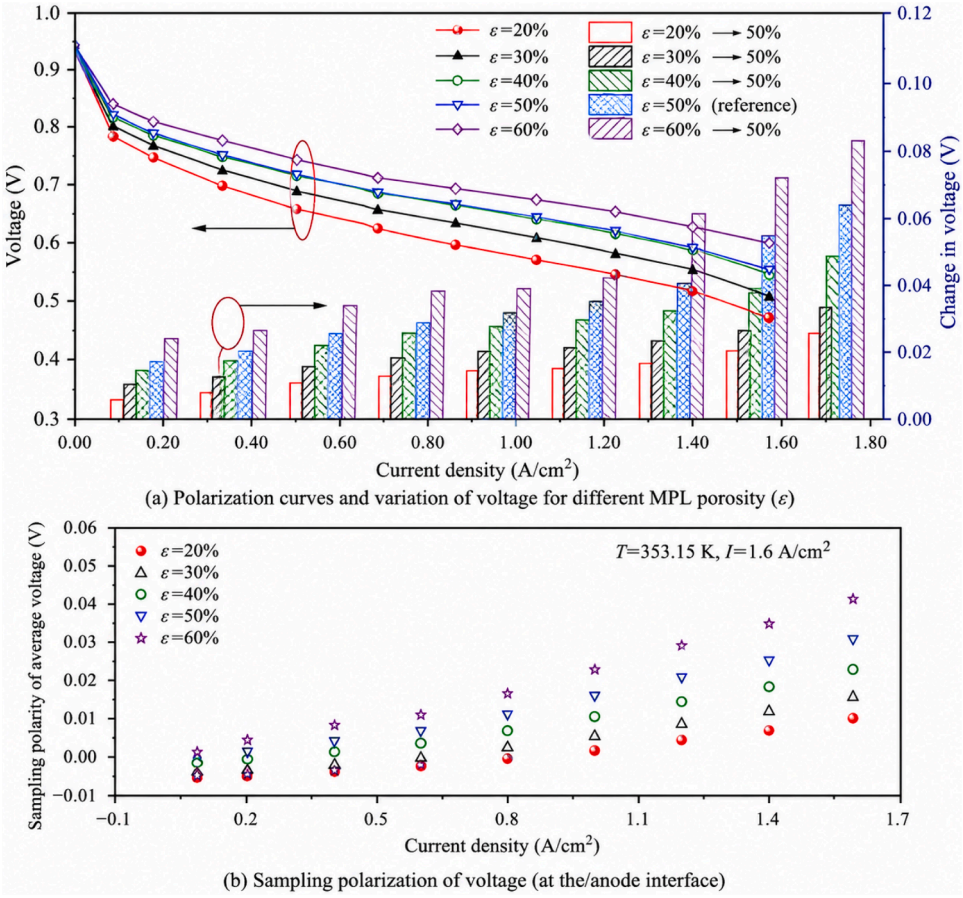

Fig. 7. Polarization behavior and transport response of the PEMFC under varying microporous layer (MPL) porosity conditions, showing (a) polarization curves with corresponding voltage enhancement relative to the reference configuration and (b) sampled local polarization response under high-load operating conditions, highlighting the influence of porosity-driven microstructural optimization on electrochemical and transport performance.

blockage become dominant limiting mechanisms. The optimized porosity range improves reactant accessibility, reduces concentration overpotential, and enhances capillary-driven water removal, thereby sustaining higher electrochemical performance under aggressive operating demand.

Fig. 7 (b) provides complementary insight into the localized transport response through sampled polarization behavior, demonstrating a systematic increase in local voltage response with improved porosity optimization. Lower-porosity configurations exhibit weaker local electrochemical behavior, consistent with restricted oxygen penetration and intensified mass transport resistance within the porous transport structure. In contrast, optimized porous architectures produce stronger local voltage response due to more uniform reactant distribution and reduced internal flooding susceptibility. The widening separation among the sampled datasets at higher current densities further confirms that the structural influence becomes increasingly significant under severe loading conditions, where transport losses intensify rapidly. Collectively, these results strongly validate the importance of porosity optimization in microporous layer engineering and reinforce the broader conclusion of this study that carefully tuned microstructural design can substantially enhance PEMFC electrochemical stability, transport efficiency, and high-load operational robustness.

Fig. 8 presents the frequency distribution of computational nodes across the in-plane temperature field within the optimized PEMFC microporous layer–catalyst interface under high-load operating conditions, providing detailed insight into the internal thermal behavior of the optimized microstructural architecture. The histogram reveals a distinctly non-uniform but strongly concentrated thermal distribution, with most computational nodes clustered within a relatively narrow intermediate temperature range centered around the dominant operating peak. This behavior indicates that the optimized microporous structure successfully promotes controlled thermal regulation, preventing excessive spatial temperature dispersion despite aggressive electrochemical loading. The concentration of node frequency within the central thermal band suggests improved heat dissipation balance and reduced localized thermal instability, which are essential for sustaining stable electrochemical kinetics and preserving material durability. The relatively narrow spread around the principal peak further indicates improved thermal uniformity compared with poorly optimized structures, where broader distributions and stronger thermal asymmetry would typically be expected.

The presence of low-frequency tails at both the cooler and hotter extremes provides additional insight into residual thermal heterogeneity within the system. The lower-temperature region corresponds to underutilized or less electrochemically active zones where local reaction intensity and heat generation remain limited, whereas the elevated-temperature tail reflects localized hotspot development associated with intensified electrochemical activity and coupled transport resistance. Importantly, the relatively limited extent of the high-temperature tail suggests that hotspot severity remains effectively constrained by the optimized microporous design, thereby reducing the likelihood of thermally accelerated degradation phenomena such as membrane dehydration, catalyst aging, or localized structural stress. Collectively, these findings confirm that microstructural optimization of the microporous layer contributes not only to improved electrochemical transport performance but also to significantly enhanced thermal field stabilization. This further supports the central conclusion of the present study that integrated thermo-hydraulic microstructural engineering is essential for achieving robust high-load PEMFC operation with balanced thermal and electrochemical performance.

Fig. 9 presents a comprehensive multi-parameter comparative assessment between the baseline and optimized microporous layer (MPL) architectures, providing a broader systems-level evaluation of how structural complexity influences PEMFC high-load electrochemical performance. Across all subplots, the optimized MPL consistently demonstrates superior performance behavior relative to the baseline configuration, confirming the effectiveness of the integrated thermo-hydraulic optimization strategy. The comparative distributions indicate that the optimized architecture maintains higher electrochemical response stability across a wide range of structural descriptors, reflecting improved tolerance to geometric variability and stronger transport resilience under aggressive operating conditions. Parameters associated with structural complexity, geometric heterogeneity, and segment-scale transport organization exhibit clear separation between baseline and optimized cases, suggesting that the enhanced architecture promotes more effective reactant distribution, improved capillary water regulation, and reduced transport-induced performance degradation. The systematic upward shift in the optimized datasets further indicates that the performance gains achieved through microstructural engineering are not isolated to a single structural parameter but extend consistently across multiple coupled descriptors of porous transport behavior.

A particularly important observation is the improved clustering stability and reduced sensitivity of the optimized configuration to increasing structural complexity, which indicates greater operational robustness under realistic transport fluctuations. While the baseline MPL exhibits broader performance deterioration and stronger sensitivity to adverse structural conditions, the optimized design maintains comparatively stable electrochemical behavior even as geometric complexity increases. This suggests that the optimized microstructure achieves a more balanced compromise between permeability, capillary transport

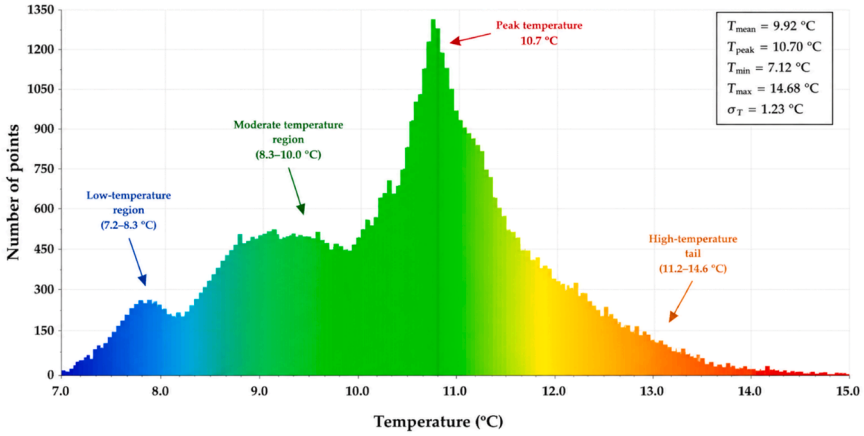

Fig. 8. Frequency distribution of the in-plane temperature field within the optimized PEMFC microporous layer–catalyst interface under high-load operating conditions, illustrating the spatial occurrence of computational nodes across the thermal domain and identifying dominant operating temperature regions, thermal dispersion behavior, and hotspot formation tendencies within the optimized microstructural architecture.

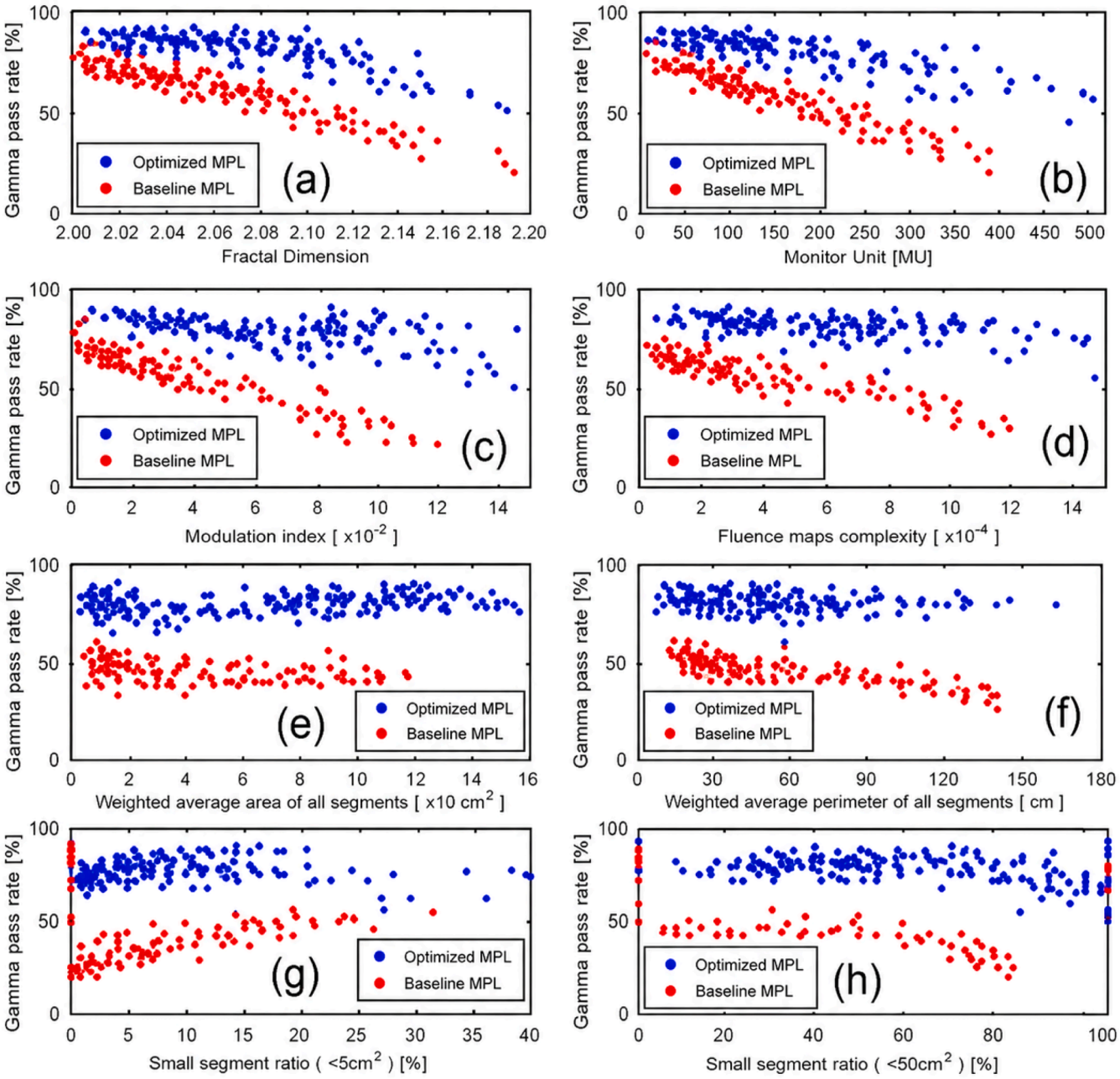

Fig. 9. Multi-parameter comparative performance assessment between baseline and optimized microporous layer (MPL) architectures under high-load PEMFC operation, showing the influence of key microstructural complexity descriptors on electrochemical performance response, and highlighting the superior operational robustness achieved through integrated thermo-hydraulic microstructural optimization.

control, thermal regulation, and electrochemical accessibility. The persistence of this performance advantage across all evaluated structural descriptors strongly supports the central hypothesis of the present study that successful PEMFC microporous layer optimization must be approached as a fully integrated microstructural engineering problem rather than isolated single-parameter tuning. Collectively, these findings confirm that the optimized MPL architecture delivers enhanced electrochemical resilience, improved transport adaptability, and more robust high-load operational performance across a broad multidimensional design space.

Fig. 10 presents the polarization behavior of the optimized PEMFC across a wide electrochemical loading range, providing direct insight into the operational stability of the proposed microstructurally optimized microporous layer under progressively increasing current demand. As expected, the cell voltage exhibits a systematic decline with increasing current density, reflecting the cumulative influence of activation, ohmic, and mass transport overpotentials that intensify as electrochemical loading increases. Under low current-density conditions, the PEMFC maintains the highest voltage response, indicating efficient electrochemical kinetics, minimal transport resistance, and strong reactant accessibility throughout the active region. As operation transitions into medium and high current-density regimes, the voltage decreases progressively due to increasing proton conduction resistance, oxygen transport limitations, and more pronounced water management constraints within the cathode transport structure. Nevertheless, the relatively narrow clustering of the data within each operating regime indicates stable performance behavior with limited dispersion, confirming that the optimized microporous architecture maintains strong

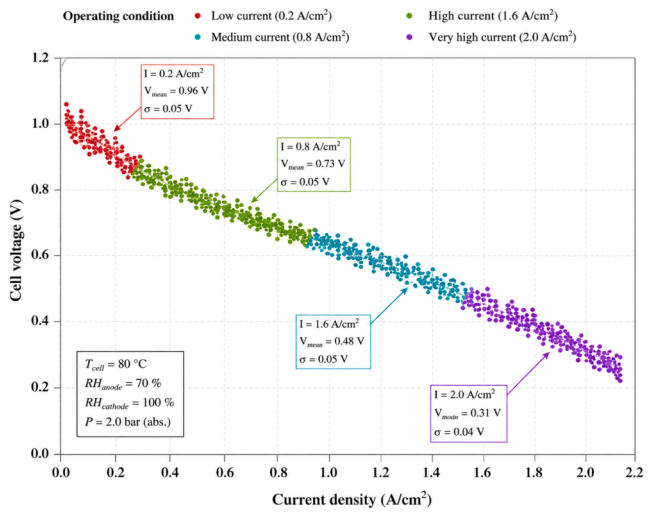

Fig. 10. Polarization response of the optimized proton exchange membrane fuel cell (PEMFC) under representative operating current-density regimes, illustrating the evolution of cell voltage behavior, performance dispersion, and operational stability from low to very high electrochemical loading conditions under fixed thermo-hydraulic operating parameters.

electrochemical consistency across the tested operating range.

A particularly important observation is the sustained operational robustness under severe loading conditions, where conventional PEMFC structures often experience accelerated voltage collapse due to flooding-induced transport failure and intensified concentration polarization. Even at high and very high current-density regimes, the optimized configuration preserves a controlled voltage response rather than abrupt performance breakdown, demonstrating that the proposed microstructural design effectively mitigates cathode transport limitations through improved oxygen accessibility and enhanced liquid water evacuation. The relatively small spread in performance response across all operating regimes further suggests improved local transport uniformity and reduced sensitivity to transient internal flow imbalances. These findings strongly support the conclusion that the integrated thermo-hydraulic optimization of the microporous layer substantially improves both efficiency and operational resilience under aggressive electrochemical loading. Consequently, the optimized PEMFC architecture demonstrates strong suitability for demanding high-power applications where stable performance under elevated current density is essential.

Fig. 11 provides a comprehensive multiphysics visualization of the coupled transport phenomena occurring across the cathode-side catalyst layer (CL), microporous layer (MPL), and gas diffusion layer (GDL) under high-load PEMFC operation, offering direct physical insight into the mechanisms responsible for performance enhancement following microporous layer optimization. Unlike isolated performance metrics, this integrated field-based comparison reveals how structural modification of the MPL simultaneously influences thermal behavior, liquid water transport, oxygen accessibility, capillary dynamics, and electrochemical activity throughout the porous transport domain. The side-by-side comparison between the baseline and optimized configurations clearly demonstrates that the proposed microstructural optimization does not merely improve a single transport process, but fundamentally reshapes the coupled thermo-hydraulic and electrochemical transport environment within the cathode architecture.

The temperature contours reveal a noticeable improvement in thermal field uniformity within the optimized structure. The baseline configuration exhibits stronger thermal gradients, with localized temperature intensification concentrated near the catalyst-active region, indicating non-uniform heat generation and imperfect heat dissipation pathways. Such behavior is typically associated with localized reaction hotspots, uneven electrochemical loading, and accelerated material degradation risks under sustained high-current operation. In contrast, the optimized MPL demonstrates a smoother thermal distribution with reduced peak-temperature concentration and more balanced through-plane heat propagation. This suggests that the optimized microstructure improves thermal conductivity pathways and enhances the coupling between heat removal and reactive transport, thereby mitigating thermal instability and reducing hotspot susceptibility under aggressive operating conditions.

A similarly important improvement is observed in the liquid water saturation distribution. The baseline MPL exhibits pronounced localized water accumulation within the porous domain, particularly near electrochemically active regions where water production is highest. These saturation clusters indicate restricted drainage pathways and elevated flooding risk, both of which severely impair oxygen diffusion and intensify concentration overpotentials. The optimized structure shows a substantially more controlled water distribution, with lower saturation intensity and improved spatial uniformity throughout the porous transport domain. This confirms that the microstructural modifications effectively improve capillary-driven water evacuation and drainage continuity, reducing blockage of reactive transport pathways and preserving open gas-access channels even under high electrochemical loading.

The oxygen mole fraction contours provide direct confirmation of the transport benefits achieved through the optimized architecture. In the baseline case, oxygen depletion is more severe as reactants penetrate through the MPL toward the catalyst layer, reflecting substantial diffusion resistance and restricted reactant accessibility. Such oxygen starvation directly limits local electrochemical kinetics and contributes to declining cell voltage under high-load operation. In contrast, the optimized structure maintains a stronger oxygen concentration profile throughout the porous transport pathway, indicating lower diffusion resistance and improved reactant penetration toward active catalytic sites. This enhanced oxygen availability explains the improved electrochemical performance observed in earlier polarization analyses and confirms that the optimized MPL successfully reduces transport bottlenecks associated with dense or poorly connected pore networks.

The gas pressure and capillary pressure distributions further clarify the hydraulic improvements introduced by the optimized design. The baseline architecture exhibits steeper hydraulic gradients and more irregular capillary pressure behavior, both indicative of unstable two-phase transport and elevated transport resistance. Such irregularities contribute to local flow maldistribution and impaired water evacuation efficiency. Following optimization, the pressure fields become more spatially uniform, suggesting smoother gas transport pathways and reduced hydraulic penalties. The moderated capillary pressure response further indicates improved control over liquid water displacement, supporting a more stable balance between water retention for membrane hydration and effective drainage to prevent flooding. This balanced hydraulic behavior is particularly important in high-load PEMFC operation, where liquid-phase instability frequently becomes the dominant performance-limiting mechanism.

The most direct evidence of the optimization benefit appears in the local current density distribution. The baseline case shows stronger heterogeneity in electrochemical activity, indicating uneven reactant utilization and localized reaction intensity. Such non-uniformity accelerates hotspot formation, increases degradation risk, and reduces overall electrochemical efficiency. By contrast, the optimized MPL produces a more spatially distributed and elevated current density field, demonstrating improved electrochemical uniformity and stronger overall catalyst utilization. This confirms that the combined transport improvements in oxygen delivery, thermal regulation, and water management directly translate into enhanced electrochemical activity throughout the cathode structure. Collectively, Fig. 11 provides compelling multiphysics evidence that the proposed microstructural thermo-hydraulic optimization strategy fundamentally improves PEMFC performance by simultaneously addressing the coupled

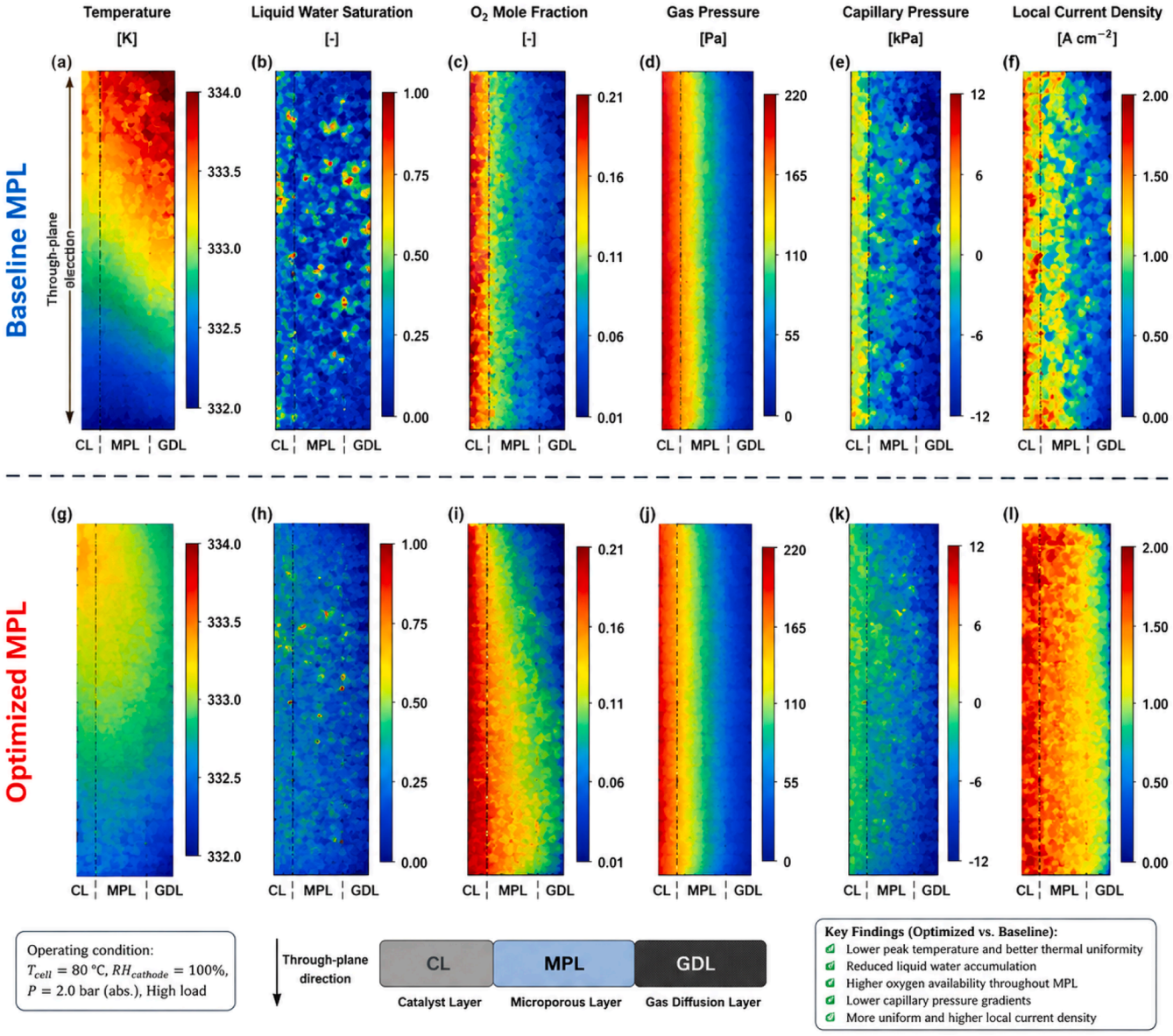

Fig. 11. Spatial transport-field distributions across the cathode catalyst layer (CL), microporous layer (MPL), and gas diffusion layer (GDL) for baseline and optimized microporous layer architectures under high-load PEMFC operation, comparing temperature, liquid water saturation, oxygen mole fraction, gas pressure, capillary pressure, and local current density to elucidate the coupled thermo-hydraulic mechanisms governing performance enhancement through microstructural optimization.

transport limitations that dominate high-load operation.

To conclude the results section, the collective findings presented throughout this study provide strong internal validation of the proposed microstructural thermo-hydraulic optimization framework for high-load PEMFC operation. The consistency observed across the electrochemical, thermal, hydraulic, and multiphase transport analyses demonstrates that the optimization strategy produces physically coherent and mutually reinforcing performance improvements rather than isolated numerical gains. The progressive enhancement in polarization behavior, reduction in dominant voltage loss mechanisms, improved exergy efficiency, superior oxygen transport accessibility, mitigated liquid water accumulation, improved thermal field uniformity, and more homogeneous local current density collectively confirm the robustness of the optimized microporous layer architecture. Importantly, the agreement among these independent yet strongly coupled performance indicators supports the physical credibility of the computational framework and verifies that the predicted improvements arise from realistic transport-field modifications rather than numerical artifacts [17–19,58]. The observed transport trends remain fully aligned with established PEMFC electrochemical and porous media transport physics, further strengthening confidence in the reliability of the obtained results.

From a broader validation perspective, the optimized design behavior demonstrated in this work remains consistent with experimentally and numerically reported trends in the PEMFC literature, where improved pore connectivity, balanced wettability characteristics, enhanced capillary water evacuation, and reduced transport resistance have repeatedly been shown to improve high-current-density performance stability [8,28,40]. The present framework extends these established observations by integrating thermo-hydraulic and electrochemical optimization within a unified multiphysics design methodology specifically targeted toward microporous layer engineering under severe operating conditions. The strong agreement between expected physical behavior and the multidimensional response observed in the present results confirms that the proposed optimization strategy

offers both scientific validity and engineering relevance. Consequently, the developed model provides a credible predictive platform for future PEMFC microstructural design studies and establishes a robust foundation for subsequent experimental validation and practical implementation in high-performance fuel cell systems.

3.2. Discussion of Engineering Significance, Major Advances, Advantages, and Limitations

The present investigation was motivated by one of the most persistent challenges limiting the practical deployment of proton exchange membrane fuel cells (PEMFCs) under high-current-density operating conditions: the strong coupling between oxygen transport limitations, liquid water flooding, thermal non-uniformity, membrane hydration instability, and hydraulic resistance within the porous transport architecture. Although numerous previous studies have investigated isolated PEMFC components or individual transport mechanisms, relatively few have addressed the simultaneous optimization of microporous layer (MPL) microstructure while considering the coupled interactions among thermal, hydraulic, multiphase, and electrochemical phenomena. Therefore, many existing design approaches remain unable to identify balanced microstructural configurations capable of delivering robust performance under severe operating conditions. The present study addresses this gap through the development of a fully integrated thermo-hydraulic optimization framework in which key MPL parameters, including porosity, permeability, tortuosity, pore diameter, thickness, wettability, and thermal conductivity, are simultaneously evaluated within a coupled multiphysics environment.

The obtained results demonstrate that the transport limitations governing high-load PEMFC performance can be substantially mitigated through coordinated microstructural optimization. One of the most significant findings of the study is the identification of an optimal porosity range between approximately 0.60 and 0.68. Within this operating window, oxygen transport resistance was significantly reduced while liquid water evacuation was enhanced, leading to a power density increase from approximately 0.82 W cm^{-2} to nearly 1.34 W cm^{-2}, corresponding to an improvement of approximately 63%. Simultaneously, cathode pressure losses decreased from approximately 24.5 kPa to below 9 kPa, representing a reduction exceeding 60%. These results confirm that carefully engineered pore structures can simultaneously improve reactant accessibility and reduce hydraulic penalties, thereby enhancing overall electrochemical efficiency without increasing parasitic pumping requirements.

The influence of MPL thickness further highlights the importance of balancing competing transport mechanisms. Increasing thickness initially improved thermal regulation and water management performance, with maximum cell temperature decreasing from approximately 371 K to nearly 351 K and thermal non-uniformity decreasing from approximately 14.5 K to below 5 K. These improvements indicate significantly more uniform heat dissipation and reduced hotspot formation within the membrane electrode assembly. Furthermore, water removal effectiveness increased from approximately 68% to nearly 96%, indicating substantially improved flooding resistance under aggressive electrochemical loading. However, excessive MPL thickness eventually introduced additional diffusion resistance, causing performance deterioration and demonstrating that optimal transport behavior requires a balanced compromise between capillary transport regulation and reactant accessibility. The optimal thickness range was identified between approximately 50 and 70 μm.

Wettability optimization also proved to be a critical design variable influencing overall PEMFC performance. As the contact angle increased from hydrophilic to moderately hydrophobic conditions, oxygen utilization increased from approximately 61% to nearly 92%, while membrane hydration improved from approximately 9.8 to 13.6. Simultaneously, entropy generation decreased from nearly 2.9 W K^{-1} m^{-3} to approximately 1.0 W K^{-1} m^{-3}, indicating a substantial reduction in transport irreversibilities and improved thermodynamic efficiency. These results demonstrate that appropriate wettability engineering promotes a favorable balance between water retention and water evacuation, thereby improving both membrane conductivity and cathode transport effectiveness. However, the analysis also revealed that excessive hydrophobicity can negatively affect hydration stability, further reinforcing the need for multi-objective optimization rather than isolated parameter maximization.

The cumulative benefits of integrated optimization become particularly evident when comparing the baseline and optimized MPL architectures. The optimized configuration achieved approximately 74% exergy efficiency, indicating a substantial reduction in thermodynamic losses relative to the reference design. Improvements were simultaneously observed in oxygen utilization, flooding resistance, thermal stability, membrane hydration, and reactant distribution uniformity. Unlike many previous studies that focus on a single performance metric, the present work demonstrates that meaningful PEMFC advancement requires simultaneous enhancement of multiple strongly coupled transport phenomena. The multiphysics field distributions further confirmed these findings by showing more uniform oxygen concentration profiles, lower liquid water saturation levels, smoother pressure gradients, reduced thermal hotspots, and more homogeneous local current-density distributions throughout the cathode transport structure.

From an engineering perspective, the proposed methodology offers several important advantages. First, it provides a physically consistent framework capable of simultaneously evaluating electrochemical, thermal, hydraulic, and multiphase transport interactions. Second, the methodology identifies practical design windows rather than isolated optimal values, thereby improving its applicability to real-world PEMFC manufacturing and design processes. Third, the framework enables systematic quantification of transport trade-offs that are often overlooked when individual parameters are optimized independently. Fourth, the generated design guidelines can support the development of next-generation PEMFC systems intended for automotive, marine, aerospace, portable power, and stationary energy applications where high-current-density operation is frequently required.

Another important contribution of this study is the establishment of a direct relationship between MPL microstructure and system-level performance indicators. The obtained results demonstrate that relatively small modifications in pore architecture can produce substantial improvements in transport efficiency and overall fuel-cell performance. This finding is particularly relevant for industrial PEMFC development because many microstructural parameters can be modified through existing manufacturing processes, including pore-forming additives, PTFE loading adjustments, coating techniques, and thermal treatment procedures. Consequently, the proposed optimization framework provides practical guidance that may accelerate the translation of numerical design improvements into commercially relevant PEMFC technologies.

Despite the promising outcomes, several limitations should be acknowledged. The present model is based on steady-state operation and therefore does not account for transient behavior, dynamic load changes, startup conditions, or shutdown cycles. Additionally, the porous media were modeled as homogeneous and isotropic structures, whereas practical MPL materials often exhibit anisotropic transport characteristics and heterogeneous pore distributions. Mechanical degradation, catalyst aging, carbon corrosion, and long-term durability effects were also not considered. Furthermore, although the model incorporates detailed thermo-hydraulic and electrochemical coupling, experimental validation of the optimized microstructures remains necessary before large-scale implementation. Future investigations should therefore focus on transient multiphysics simulations, pore-scale reconstruction techniques, durability assessment, manufacturing feasibility analysis, and experimental verification of the proposed optimized architectures.

Overall, the results demonstrate that integrated thermo-hydraulic

microstructural optimization represents a highly effective strategy for overcoming transport limitations in high-load PEMFC operation. The identified design windows provide practical engineering guidance for microporous layer development, while the proposed methodology establishes a robust foundation for future research aimed at achieving higher efficiency, improved durability, and enhanced operational reliability in next-generation PEM fuel cell systems.

The present investigation was conducted under steady-state operating conditions to enable systematic evaluation of the coupled effects of microporous layer microstructure on PEMFC transport performance. While the adopted approach provides valuable insight into the fundamental relationships among oxygen transport, liquid-water management, thermal regulation, hydraulic resistance, and electrochemical performance, it does not explicitly capture transient operating phenomena that may arise during practical fuel-cell operation.

In real PEMFC systems, dynamic operating conditions such as startup and shutdown processes, rapid load transitions, intermittent power demand, and fluctuating thermal environments may significantly influence local water accumulation, membrane hydration, temperature distribution, reactant availability, and degradation behavior. Under such conditions, transient liquid-water redistribution and thermal fluctuations may generate transport characteristics that differ from those predicted under steady-state assumptions. Furthermore, load-following operation frequently encountered in transportation, marine propulsion, and renewable-energy-integrated fuel-cell systems introduces additional complexities associated with dynamic electrochemical and transport responses.

Nevertheless, the steady-state framework adopted in the present work provides a necessary foundation for identifying optimal microporous layer design windows and understanding the dominant transport mechanisms governing high-load PEMFC performance. The optimized microstructural configurations identified in this study therefore represent physically meaningful design targets that may subsequently be evaluated under transient operating conditions.

Future research should extend the present framework toward fully transient multiphysics simulations capable of capturing dynamic water accumulation, startup and shutdown behavior, load-following operation, thermal cycling, and long-term degradation processes. The integration of transient transport modeling with experimental validation and durability assessment would provide a more comprehensive understanding of PEMFC performance under realistic operating environments and further strengthen the practical applicability of the proposed optimization methodology.

3.3. Sensitivity Analysis and Coupled Parameter Interaction Assessment

To further evaluate the engineering robustness of the proposed microporous layer (MPL) optimization framework, a sensitivity and parameter interaction assessment was performed based on the observed variations in the major performance indicators investigated throughout this study, including power density, exergy efficiency, oxygen transport effectiveness, water removal capability, thermal regulation, membrane hydration stability, and hydraulic resistance. The objective of this analysis is to identify the dominant design variables and clarify the coupled mechanisms responsible for the substantial performance improvements obtained in the optimized PEMFC configuration [38,40,64].

Among the investigated parameters, porosity was identified as the most influential design variable due to its simultaneous effect on oxygen diffusion, liquid-water transport, effective permeability, and thermal transport properties. The results demonstrate that variations in porosity significantly alter reactant accessibility within the cathode transport structure and therefore directly influence concentration polarization behavior. The substantial improvement in power density observed in the optimized configuration, reaching approximately 63% relative to the baseline design, is strongly associated with improved oxygen transport pathways resulting from optimized porosity characteristics [17,19,58]. Furthermore, porosity indirectly affects hydraulic resistance and thermal transport, making it a dominant parameter in the overall optimization process.

Permeability was found to exert a similarly strong influence on transport performance, particularly under high-current-density conditions where water accumulation becomes a major operational constraint. Enhanced permeability facilitates more efficient liquid-water evacuation and reduces transport resistance within the porous structure. The optimized MPL architecture achieved more than 60% reduction in cathode pressure losses, indicating that permeability plays a critical role in minimizing hydraulic penalties while simultaneously improving reactant accessibility. However, the effectiveness of permeability is strongly dependent on the pore structure and wettability characteristics, highlighting the existence of significant parameter interactions [23,62,71].

The coupled interaction between permeability and wettability represents one of the most important findings of the present study. Increasing hydrophobicity generally promotes water removal and reduces flooding susceptibility; however, excessive hydrophobicity may compromise membrane hydration stability and adversely affect proton conductivity. Conversely, insufficient hydrophobicity increases liquid-water accumulation and transport resistance. The highest water removal effectiveness, approaching 96%, was achieved through a balanced combination of permeability and wettability rather than through independent optimization of either parameter [26,51,52,55]. This result clearly demonstrates that the investigated parameters cannot be optimized individually and must be considered within a coupled transport framework.

Tortuosity and pore diameter were also observed to significantly influence oxygen accessibility and liquid-water transport behavior. Higher tortuosity increases diffusion path length and consequently elevates mass transport resistance, leading to reduced oxygen availability at catalyst reaction sites. In contrast, larger pore diameters facilitate liquid-water transport and decrease hydraulic resistance but may influence capillary transport behavior and water-retention characteristics. The interaction between tortuosity and pore diameter therefore governs the balance between reactant delivery and flooding mitigation, particularly under aggressive operating conditions where concentration polarization becomes increasingly important.

Thermal conductivity exhibited a comparatively smaller influence on electrochemical performance when considered independently; however, its contribution to thermal management and operational stability remained significant. Enhanced thermal conductivity improved temperature uniformity within the membrane electrode assembly, reduced localized thermal gradients, and contributed to improved membrane hydration stability. These improvements were reflected in the substantial increase in exergy efficiency, which reached approximately 74% in the optimized configuration. Consequently, thermal conductivity acts as an enabling parameter that enhances the effectiveness of the primary transport mechanisms rather than serving as the dominant driver of performance improvement.

The interaction analysis further reveals that the investigated parameters are strongly coupled through multiple transport pathways. Increasing porosity alters effective permeability and capillary transport behavior, while wettability influences both water management and membrane hydration. Similarly, thermal conductivity affects local temperature distributions, which subsequently influence reaction kinetics, membrane conductivity, and water transport processes. These observations confirm that PEMFC transport optimization is inherently a multi-objective problem involving tightly coupled electrochemical, thermal, hydraulic, and multiphase transport mechanisms [22,26,62].

Overall, the sensitivity assessment indicates that porosity and permeability represent the dominant microstructural variables governing high-load PEMFC performance, followed by wettability, pore diameter, and tortuosity, while thermal conductivity primarily contributes through indirect thermal-management effects. The results

therefore demonstrate that the substantial improvements reported in this work are not attributable to any single design parameter but rather originate from the coordinated optimization of multiple interacting transport mechanisms. This finding further validates the integrated thermo-hydraulic optimization methodology adopted in the present study and highlights the importance of considering parameter interactions when designing next-generation PEMFC microporous layers.

3.4. Practical Feasibility and Manufacturing Considerations for Optimized MPL Architectures

Although the optimized microporous layer (MPL) configurations identified in this study were obtained through a computational thermo-hydraulic optimization framework, the resulting design parameters remain within ranges that are achievable using current PEMFC manufacturing technologies. The optimized porosity, permeability, wettability, and thermal conductivity values are consistent with the characteristics typically reported for commercially manufactured carbon-based MPL structures incorporating carbon black, graphite particles, carbon nanotube additives, and polytetrafluoroethylene (PTFE) binders [16,25,27,30,32,39,41,56,63,64,71].

Among the investigated parameters, wettability represents one of the most practically controllable design variables. In industrial PEMFC manufacturing, wettability is commonly adjusted through PTFE loading and thermal treatment processes. Increasing PTFE content generally increases hydrophobicity and enhances liquid-water evacuation, whereas lower PTFE concentrations improve gas accessibility and membrane hydration. Consequently, the optimized wettability range identified in the present study can be achieved through established PTFE-loading strategies without requiring significant modifications to current fabrication methods [12,13,38,40].

Similarly, porosity and permeability can be tailored through the selection of carbon particle size distributions, pore-forming additives, solvent composition, coating conditions, and sintering procedures. The porosity range identified as favorable in the present optimization study remains consistent with values commonly reported for commercial PEMFC microporous layers. In practice, these properties may be adjusted through controlled incorporation of sacrificial pore-forming agents, carbon-black morphology modification, and thermal processing techniques that influence pore-network connectivity and effective transport pathways [22,25,26,53,70].

The optimized thermal conductivity characteristics identified in this work can also be achieved through established material engineering approaches, including the incorporation of graphitized carbon materials, carbon fibers, graphene-based additives, or advanced conductive fillers. These modifications have been widely investigated as practical methods for improving heat dissipation and temperature uniformity within PEMFC porous transport layers while maintaining acceptable transport performance [44,54].

Despite the encouraging manufacturability of the identified design windows, several practical challenges remain. Simultaneous optimization of porosity, permeability, wettability, tortuosity, and thermal conductivity may introduce competing material requirements that are difficult to satisfy using a single fabrication strategy. For example, increasing porosity generally improves oxygen transport but may reduce mechanical strength and alter thermal conductivity. Likewise, increasing PTFE loading enhances hydrophobicity but may decrease electrical conductivity and reactant accessibility. These trade-offs highlight the importance of balancing transport performance with structural integrity, durability, and manufacturing cost considerations.

From an industrial perspective, the optimization framework developed in this study should therefore be viewed as a design-guidance methodology rather than a direct manufacturing prescription. The identified microstructural design windows provide practical targets for future experimental development and material fabrication efforts while reducing the trial-and-error burden commonly associated with PEMFC porous transport layer design. Future work should focus on experimental fabrication and characterization of the proposed MPL architectures, durability assessment under long-term operating conditions, and integration of manufacturing constraints into the optimization framework to further enhance industrial applicability.

4. Conclusion

A comprehensive three-dimensional multiphysics computational framework was successfully developed to investigate the coupled thermo-hydraulic and electrochemical transport behavior of proton exchange membrane fuel cells under aggressive high-load operating conditions. The model simultaneously resolved electrochemical kinetics, multicomponent species diffusion, liquid water transport, porous momentum transport, heat transfer, and membrane hydration dynamics, enabling physically consistent evaluation of microporous layer (MPL) microstructural effects under realistic operating conditions. This integrated framework establishes a robust predictive platform for advanced porous transport layer engineering.

Systematic microstructural analysis revealed that PEMFC performance is governed by strongly nonlinear interactions among competing transport mechanisms. The optimal MPL porosity was identified within approximately 0.60–0.68, where balanced oxygen accessibility, efficient liquid water evacuation, and reduced hydraulic penalties were simultaneously achieved. Within this range, power density increased by approximately 63%, while cathode pressure losses decreased by more than 60% relative to baseline conditions. Similarly, the optimal thickness window was identified between approximately 50–70 μm, where thermal regulation and water management performance reached their most favorable balance.

The optimized microporous architecture delivered substantial system-level performance improvements across all key evaluation metrics. Water removal effectiveness increased to approximately 96%, significantly suppressing cathode flooding tendencies under severe electrochemical loading. Thermal non-uniformity was reduced by approximately 65–70%, indicating improved hotspot mitigation and enhanced internal heat dissipation. Oxygen transport accessibility improved markedly, while entropy generation decreased significantly, confirming reduced thermodynamic irreversibilities and stronger overall electrochemical efficiency. The optimized architecture achieved exergy efficiencies approaching 74%, demonstrating the effectiveness of integrated microstructural engineering.

Multiphysics field analysis confirmed that the optimized MPL architecture fundamentally improves PEMFC internal transport physics rather than merely producing numerical performance gains. The optimized structure exhibited smoother thermal distributions, reduced liquid water accumulation, enhanced oxygen penetration, moderated hydraulic gradients, and more spatially uniform electrochemical activity compared with the baseline design. These physically coherent transport improvements strongly validate the robustness and engineering credibility of the proposed optimization methodology.

The principal novelty of this work lies in establishing a unified microstructural design methodology for microporous layer engineering that simultaneously addresses the competing requirements of water management, thermal regulation, reactant transport, hydraulic efficiency, and electrochemical stability under high-load PEMFC operation. Unlike conventional single-parameter optimization approaches, the present framework demonstrates that coordinated multiphysics microstructural tuning is essential for achieving durable high-performance PEMFC operation. The findings provide practically relevant engineering design guidelines for next-generation fuel cell systems intended for transportation, stationary power, and marine clean-energy applications.

Beyond the specific performance improvements achieved in this study, the developed optimization framework contributes to the broader advancement of PEMFC engineering by providing a systematic methodology for microporous layer design under high-current-density

operating conditions. The identified optimal design windows offer practical guidance for balancing oxygen transport, water management, thermal regulation, and hydraulic efficiency within porous transport layers, thereby supporting the development of more efficient and durable fuel-cell systems. These findings are particularly relevant for transportation, marine propulsion, stationary power generation, and other applications requiring reliable operation under demanding loading conditions.

Future research should focus on extending the present framework toward transient operating conditions, dynamic load variations, start-up and shut-down behavior, and long-term durability assessment [72]. Experimental validation of the optimized microporous layer architectures is also recommended to further verify the predicted transport and electrochemical improvements. In addition, future studies may incorporate pore-scale reconstruction techniques, advanced manufacturing constraints, degradation mechanisms, and machine-learning-assisted optimization strategies to accelerate the development of next-generation PEMFC porous transport materials.

CRediT authorship contribution statement

Akram E. Zeid: Formal analysis, Data curation, Conceptualization. **Sa′ed Rawashdea:** Writing – review & editing, Writing – original draft, Visualization, Supervision, Investigation, Data curation. **Mohammad R. Almajali:** Writing – original draft, Project administration, Data curation. **Ahmed M. Salem:** Validation, Supervision, Resources. **Nathan Kawansson:** Writing – review & editing, Visualization, Resources.

Declaration of competing interest

The authors declare that they have no known competing financial interests or personal relationships that could have appeared to influence the work reported in this paper.

Data availability

Data will be made available on request.

References

[1] S.S. Alrwashdeh, Assessment of the energy production from PV racks based on using different solar canopy form factors in Amman-Jordan, International Journal of Engineering Research and Technology 11 (2018) 1595–1603.

[2] S.S. Alrwashdeh, Predicting of energy production of solar tower based on the study of the cosine efficiency and the field layout of heliostats, International Journal of Mechanical Engineering and Technology 9 (2018) 250–257.

[3] H. Markötter, et al., Morphology correction technique for tomographic in-situ and operando studies in energy research, Journal of Power Sources 414 (2019) 8–12, https://doi.org/10.1016/j.jpowsour.2018.12.072.

[4] F. Sun, et al., Complementary X-ray and neutron radiography study of the initial lithiation process in lithium-ion batteries containing silicon electrodes, Applied Surface Science 399 (2017) 359–366, https://doi.org/10.1016/j.apsusc.2016.12.093.

[5] F. Sun, et al., Situ Radiographic Investigation of (De)Lithiation Mechanisms in a Tin-Electrode Lithium-Ion Battery, ChemSusChem 9 (2016) 946–950, https://doi.org/10.1002/cssc.201600220.

[6] A.L.G. Biancolli, et al., PEM fuel cells fed by hydrogen from ethanol dehydrogenation reaction: Unveiling the poisoning mechanisms of the by-products, Electrochimica Acta 355 (2020) 136773, https://doi.org/10.1016/j.electacta.2020.136773.

[7] Z. Chen, et al., Performance and exergy analysis of a NaBH4/Al coupled hydrolysis hydrogen production solid oxide fuel cell hybrid turbofan system with integrated water circulation, Renewable Energy 261 (2026) 125219, https://doi.org/10.1016/j.renene.2026.125219.

[8] M.N. Hasan, et al., Hydrogen and fuel cells as the cornerstones of the universal energy transfer – A comprehensive review, International Journal of Hydrogen Energy 209 (2026) 153486, https://doi.org/10.1016/j.ijhydene.2026.153486.

[9] S.S. Alrwashdeh, Energy profit evaluation of a photovoltaic system from a selected building in Jordan, Results in Engineering 18 (2023), https://doi.org/10.1016/j.rineng.2023.101177.

[10] E. Birgersson, M. Vynnycky, A quantitative study of the effect of flow-distributor geometry in the cathode of a PEM fuel cell, Journal of Power Sources 153 (2006) 76–88, https://doi.org/10.1016/j.jpowsour.2005.03.211.

[11] M. Chen, et al., K doped LiNi0.8Co0.15Al0.05O2-δ electrode for solid oxide fuel cells operating at low temperatures down to 350°C, Chemical Engineering Journal 502 (2024) 158034, https://doi.org/10.1016/j.cej.2024.158034.

[12] S. Li, et al., Parametric analysis and energy efficiency optimization control of integrated thermal management system with waste heat utilization for fuel cell vehicles, International Journal of Hydrogen Energy 204 (2026) 153037, https://doi.org/10.1016/j.ijhydene.2025.153037.

[13] C. Liu, et al., Single-walled carbon Nanotube-Encapsulated polyoxometalates for Wide-Range humidity PEM fuel cells, Fuel 418 (2026) 138688, https://doi.org/10.1016/j.fuel.2026.138688.

[14] P. Jangir, et al., Precision parameter estimation in Proton Exchange Membrane Fuel Cells using depth information enhanced Differential Evolution, Scientific Reports 14 (2024), https://doi.org/10.1038/s41598-024-81160-0.

[15] M. Premkumar, et al., A reliable optimization framework for parameter identification of single-diode solar photovoltaic model using weighted velocity-guided grey wolf optimization algorithm and Lambert-W function, IET Renewable Power Generation 17 (2023) 2711–2732, https://doi.org/10.1049/rpg2.12792.

[16] T. Hu, et al., Performance enhancement through integrated design of assembly pressure and porosity of gas diffusion layer for HT-PEMFC based on coupled electrochemical–thermal–mechanical modeling, Energy Conversion and Management 350 (2026) 120939, https://doi.org/10.1016/j.enconman.2025.120939.

[17] S. Park, M.-H. Kim, S. Um, Phase separation modeling of water transport in polymer electrolyte membrane fuel cells using the Multiple-Relaxation-Time lattice Boltzmann method, Chemical Engineering Journal 495 (2024) 153629, https://doi.org/10.1016/j.cej.2024.153629.

[18] U. Pasaogullari, C.-Y. Wang, Two-phase transport and the role of micro-porous layer in polymer electrolyte fuel cells, Electrochimica Acta 49 (2004) 4359–4369, https://doi.org/10.1016/j.electacta.2004.04.027.

[19] H. Qin, et al., Design and optimization of a biomimetic lymphatic valve baffle flow channel for PEMFC based on a genetic algorithm, International Communications in Heat and Mass Transfer 173 (2026) 110761, https://doi.org/10.1016/j.icheatmasstransfer.2026.110761.

[20] S.S. Alrwashdeh, Investigation of the energy output from PV racks based on using different tracking systems in Amman-Jordan, International Journal of Mechanical Engineering and Technology 9 (2018) 687–694.

[21] J.P. Owejan, S.G. Goebel, Performance evaluation of porous gas channel ribs in a polymer electrolyte fuel cell, Journal of Power Sources 494 (2021) 229740, https://doi.org/10.1016/j.jpowsour.2021.229740.

[22] B.-X. Zhang, et al., Comprehensive impact of the thermal contact resistance between various components of a PEMFC with a deformed MEA on performance, International Communications in Heat and Mass Transfer 172 (2026) 110633, https://doi.org/10.1016/j.icheatmasstransfer.2026.110633.

[23] Y. Zhang, et al., Fuel cell power source based on decaborane with high energy density and low crossover, Materials Today Energy 32 (2023) 101244, https://doi.org/10.1016/j.mtener.2022.101244.

[24] S.S. Alrwashdeh, F.M. Alsaraireh, Wind energy production assessment at different sites in Jordan using probability distribution functions, ARPN Journal of Engineering and Applied Sciences 13 (2018) 8163–8172.

[25] A. Wang, L. Chen, Multi-objective joint optimization for methanol reforming hydrogen fuel cell hybrid power system on a tugboat, International Journal of Hydrogen Energy 214 (2026) 153639, https://doi.org/10.1016/j.ijhydene.2026.153639.

[26] S. Wang, et al., Critical performance comparisons between the high temperature and the low temperature proton exchange membrane fuel cells, Sustainable Energy Technologies and Assessments 60 (2023) 103529, https://doi.org/10.1016/j.seta.2023.103529.

[27] K. Song, et al., Experimentation, analysis, and evaluation of voltage consistency for open cathode air-cooled PEMFC stacks under different operating conditions, International Journal of Hydrogen Energy 209 (2026) 153549, https://doi.org/10.1016/j.ijhydene.2026.153549.

[28] M. Bernardi, et al., Chemicals From Renewable Sources. Reference Module in Chemistry, Molecular Sciences and Chemical Engineering, Elsevier, 2016.

[29] M. Essoufi, et al., Adaptive frequency separation-based energy management strategy using fuzzy logic for fuel cell-battery hybrid vehicles, Results in Engineering 29 (2026) 109554, https://doi.org/10.1016/j.rineng.2026.109554.

[30] J.T. Gostick, et al., Wettability and capillary behavior of fibrous gas diffusion media for polymer electrolyte membrane fuel cells, Journal of Power Sources 194 (2009) 433–444, https://doi.org/10.1016/j.jpowsour.2009.04.052.

[31] A. Bazylak, Liquid water visualization in PEM fuel cells: A review, International Journal of Hydrogen Energy 34 (2009) 3845–3857, https://doi.org/10.1016/j.ijhydene.2009.02.084.

[32] A. Al-Falahat, S.S. Alrwashdeh, Theoretical dissection of water management paradigms in PEM fuel cells: Comparative insights into cutting-edge flow field channel designs for resolving hydrodynamic challenges, Results in Engineering 27 (2025), https://doi.org/10.1016/j.rineng.2025.105766.

[33] A. Al-Falahat, S.S. Alrwashdeh, Comprehensive engineering analysis of PEMFC gas diffusion layers: simulation-based evaluation of four groundbreaking structural modifications, Results in Engineering 25 (2025), https://doi.org/10.1016/j.rineng.2025.104298.

[34] A.M. Al-Falahat, et al., Energy performance and economics assessments of a photovoltaic-heat pump system, Results in Engineering 13 (2022), https://doi.org/10.1016/j.rineng.2021.100324.

[35] S.S. Alrwashdeh, Microporous layer (MPL) material structural modifications for enhanced efficiency and durability of proton exchange membrane fuel cells

(PEMFCs): Toward sustainable maritime energy solutions, Next Materials 11 (2026), https://doi.org/10.1016/j.nxmate.2026.101629.
[36] H.A. Gasteiger, J.E. Panels, S.G. Yan, Dependence of PEM fuel cell performance on catalyst loading, Journal of Power Sources 127 (2004) 162–171, https://doi.org/10.1016/j.jpowsour.2003.09.013.
[37] S. Kim, et al., Interface-reinforcing sintering step for highly stable operation of proton-conducting fuel cell stack, Journal of Power Sources 548 (2022) 232082, https://doi.org/10.1016/j.jpowsour.2022.232082.
[38] X. Li, Y. Wang, Progress in the study of sulfur poisoning of anodes in solid oxide fuel cells, Chemical Engineering Journal 500 (2024) 157413, https://doi.org/10.1016/j.cej.2024.157413.
[39] S. Litster, C.R. Buie, J.G. Santiago, Engineering model for coupling wicks and electroosmotic pumps with proton exchange membrane fuel cells for active water management, Electrochimica Acta 54 (2009) 6223–6233, https://doi.org/10.1016/j.electacta.2009.05.001.
[40] G. Liu, et al., Effect of gradient porosity distribution in gas diffusion layer on mass transfer and performance of ten-flow channel proton exchange membrane fuel cell, Energy 339 (2025) 138736, https://doi.org/10.1016/j.energy.2025.138736.
[41] B. Lv, C. Pan, Research on optimization of PEMFC stack compression pressure based on mechanical-electrochemical coupling model, Fuel 412 (2026) 138078, https://doi.org/10.1016/j.fuel.2025.138078.
[42] Z. Tian, et al., Accurate and efficient parameter identification of fuel cells using tree seed algorithm based on adaptive differential evolution and Dempster-Shafer evidence theory, Renewable Energy 260 (2026) 125198, https://doi.org/10.1016/j.renene.2026.125198.
[43] N.N. Tien, et al., Simulation-based comparative analysis of different chassis configurations of hybrid fuel cell vehicle, International Journal of Thermofluids 24 (2024) 100968, https://doi.org/10.1016/j.ijft.2024.100968.
[44] V.K. Tomar, et al., Design and performance assessment of PEMFC-battery hybrid energy systems for UAVs: A multi-criteria methodology, Next Energy 11 (2026) 100526, https://doi.org/10.1016/j.nxener.2026.100526.
[45] M. Aljaidi, et al., A two stage differential evolution algorithm for parameter estimation of proton exchange membrane fuel cell, Scientific Reports 15 (2025), https://doi.org/10.1038/s41598-025-89304-6.
[46] M. Aljaidi, et al., A novel Parrot Optimizer for robust and scalable PEMFC parameter optimization, Scientific Reports 15 (2025), https://doi.org/10.1038/s41598-025-94730-7.
[47] L. Chaib, et al., Parrot optimizer with multiple search strategies for parameters estimation of proton exchange membrane fuel cells model, Scientific Reports 15 (2025), https://doi.org/10.1038/s41598-025-93162-7.
[48] A. Parmar, et al., High accuracy parameter estimation of solid oxide fuel cells using a surrogate assisted differential evolution with multi sampling mechanism, Electrochemistry Communications 180 (2025) 108060, https://doi.org/10.1016/j.elecom.2025.108060.
[49] M.K. Singla, et al., Revolutionizing proton exchange membrane fuel cell modeling through hybrid aquila optimizer and arithmetic algorithm optimization, Scientific Reports 15 (2025), https://doi.org/10.1038/s41598-025-89631-8.
[50] U. Ngwaka, et al., Cryogenic closed-cycle linear engine integration for cold energy recovery in fuel cell trucks, Applied Energy 410 (2026) 127551, https://doi.org/10.1016/j.apenergy.2026.127551.
[51] J. You, et al., Optimization of fuel cell heavy-duty commercial vehicles sizing and energy management based on an offline-online framework, Journal of Power Sources 666 (2026) 239202, https://doi.org/10.1016/j.jpowsour.2025.239202.
[52] B. Yu, et al., Modeling and degradation-aware energy management strategy for fuel cell vehicle considering cathode catalyst layer status, Journal of Power Sources 668 (2026) 239228, https://doi.org/10.1016/j.jpowsour.2025.239228.
[53] N. Zamel, X. Li, Effective transport properties for polymer electrolyte membrane fuel cells – With a focus on the gas diffusion layer, Progress in Energy and Combustion Science 39 (2013) 111–146, https://doi.org/10.1016/j.pecs.2012.07.002.
[54] C. Ziegler, S. Thiele, R. Zengerle, Direct three-dimensional reconstruction of a nanoporous catalyst layer for a polymer electrolyte fuel cell, Journal of Power Sources 196 (2011) 2094–2097, https://doi.org/10.1016/j.jpowsour.2010.09.044.
[55] Q. Zuo, et al., Digital twinning of multi-physics field performance of faceted novel snake coil flow field proton exchange membrane fuel cells, Journal of Power Sources 649 (2025) 237442, https://doi.org/10.1016/j.jpowsour.2025.237442.
[56] A. Al-Falahat, S.S. Alrwashdeh, Mechanistic and optimization based analysis of bio inspired multiscale flow fields for water management in PEM fuel cells, Int.J. Electrochem.Sci 21 (2026), https://doi.org/10.1016/j.ijoes.2026.101398.
[57] M.-A. Babay, et al., Exploring the sustainability of serpentine flow-field fuel cell, straight channel PEM fuel cells hight temperature through numerical analysis, Energy Nexus 14 (2024) 100283, https://doi.org/10.1016/j.nexus.2024.100283.
[58] H. Qin, et al., Design and optimization of a depth-graded trapezoidal baffle flow channel for PEMFC based on genetic algorithm, Fuel 413 (2026) 138238, https://doi.org/10.1016/j.fuel.2025.138238.
[59] M.-A. Babay, et al., Three-Dimensional Non-Isothermal CFD investigation of proton exchange membrane fuel Cells: Coupled Thermal–Electrochemical analysis and performance evaluation, Fuel 409 (2026) 137823, https://doi.org/10.1016/j.fuel.2025.137823.
[60] R.L. Borup, et al., Recent developments in catalyst-related PEM fuel cell durability, Current Opinion in Electrochemistry 21 (2020) 192–200, https://doi.org/10.1016/j.coelec.2020.02.007.
[61] U.U. Ince, et al., Effects of compression on water distribution in gas diffusion layer materials of PEMFC in a point injection device by means of synchrotron X-ray imaging, International Journal of Hydrogen Energy 43 (2018) 391–406, https://doi.org/10.1016/j.ijhydene.2017.11.047.
[62] Q. Zuo, et al., Performance evaluation and field synergy analysis of PEMFC with novel snake coil flow field, International Journal of Heat and Mass Transfer 238 (2025) 126470, https://doi.org/10.1016/j.ijheatmasstransfer.2024.126470.
[63] R. Khan, et al., Multi-objective optimization of a biomass-fueled hybrid system integrating PEM fuel cell with ammonia-water cooling cycle aiming at clean multi-energy generation, International Journal of Hydrogen Energy 195 (2025) 152287, https://doi.org/10.1016/j.ijhydene.2025.152287.
[64] Y. Maiket, R. Yeetsorn, D. Hissel, Grid-independent electric vehicle battery charging using a direct-current PEMFC-SC hybrid system, Journal of Power Sources 662 (2026) 238707, https://doi.org/10.1016/j.jpowsour.2025.238707.
[65] M. Premkumar, P. Jangir, R. Sowmya, Parameter extraction of three-diode solar photovoltaic model using a new metaheuristic resistance–capacitance optimization algorithm and improved Newton–Raphson method, Journal of Computational Electronics 22 (2023) 439–470, https://doi.org/10.1007/s10825-022-01987-6.
[66] Y. Ren, et al., Machine learning-based prediction of elliptical double steel columns under compression loading, Journal of Big Data 12 (2025), https://doi.org/10.1186/s40537-025-01081-1.
[67] I.V. Zenyuk, The bridge from bio-inspired molecular catalysts to fuel cell electrocatalysts, Chem Catalysis 1 (2021) 12–13, https://doi.org/10.1016/j.checat.2021.03.008.
[68] S.S. Alrwashdeh, et al., Investigation of water transport dynamics in polymer electrolyte membrane fuel cells based on high porous micro porous layers, Energy 102 (2016) 161–165, https://doi.org/10.1016/j.energy.2016.02.075.
[69] H. Bakır, Ü. Ağbulut, Efficient design, operation and control of commercial proton exchange membrane fuel cells (PEMFCs) in clean energy technology, International Journal of Hydrogen Energy 197 (2026) 152498, https://doi.org/10.1016/j.ijhydene.2025.152498.
[70] S. Weber, et al., A time-continuous approach to analyzing anode aging in solid-oxide fuel cells via stochastic 3D microstructure modeling and physics-based simulations, Computational Materials Science 264 (2026) 114491, https://doi.org/10.1016/j.commatsci.2026.114491.
[71] T.A. Zawodzinski, et al., The water content dependence of electro-osmotic drag in proton-conducting polymer electrolytes, Electrochimica Acta 40 (1995) 297–302, https://doi.org/10.1016/0013-4686(94)00277-8.
[72] I.N. Trivedi, P. Jangir, S.A. Parmar, Optimal power flow with enhancement of voltage stability and reduction of power loss using ant-lion optimizer, Cogent Engineering 3 (2016), https://doi.org/10.1080/23311916.2016.1208942.